PHOTOIONIZATION ION CYCLOTRON RESONANCE SPECTROSCOPY: A STUDY OF THREE C_3H_6O ISOMERS

Thesis by

John Mitchell Weigel

In Partial Fulfillment of the Requirements
for the Degree of
Master of Science

California Institute of Technology
Pasadena, California

1973
(Submitted September 18, 1972)

ACKNOWLEDGEMENTS

Thanks is given to the National Science Foundation for support for two years as a trainee. Funds were received for one year from Caltech as a graduate research assistant. My last year I was a graduate teaching assistant for Chem 1 and Chem 3, which was one of the best experiences I had at Caltech.

Thanks is given to my research advisor, Jesse Lee Beauchamp, for many ideas and some non-academic good times. Jack is very accessible to his graduate students, while allowing them to work pretty much on their own. This freedom was unfortunately not particularly helpful in my particular case, as my interest in serious research waned.

To the various members of the Beauchamp research group go thanks for help with ideas about cheristry and practical assistance in getting things running. Bob Wyatt, Peter Miasek, Terry McMahon, Doug Ridge, and Mike Foster are especially thanked.

The men in the glass, instrument, and electronics shops are thanked for much patient help and many successfully completed projects. My association with the people who really enable us to get experimental research done was one of the high points of my years at Caltech.

Acknowledgement is given to Dan Harris, without whose efforts in crashing 27J I would probably still be struggling to become a Ph. D., Deciding that the road I was on was not the best one for me was the hardest decision I faced here at Caltech.

ABSTRACT

Photoionization ion cyclotron resonance (pi-icr) spectroscopy is described in detail. The construction and use of rare gas resonance line lamps employing LiF windows is described, with principle emphasis on the argon resonance line lamp that produces photons of 11.62 and 11.83 eV. Calculations of the number density and single resonance signal intensity are made for primary, secondary, and tertiary ions, and the low pressure lineshape calculated for an unreactive primary ion.

The ion chemistry of propanal, acetone, and propylene oxide (empirical formula C_3H_6O) is investigated using pi-icr with the argon resonance line lamp. The major reaction sequence in propanal and acetone is parent ion producing protonated parent ion, which condenses with the parent neutral to produce the proton bound dimer. This is also the reaction sequence in ethylene oxide. In propylene oxide, however, the parent ion relative abundance is essentially constant from 10^{-6} to 10^{-4} torr. The fragment ion of mass 43 is the predominant primary ion at the argon resonance lines, and reacts to form ions of mass 41, 57, and 59. Double resonance is used to determine the reaction sequence of the major ions. At 10^{-4} torr, there is less than 2% of the proton bound dimer in propylene oxide, while in acetone or propanal the proton bound dimer is the major product ion. Preliminary photolysis results on propylene oxide suggest a chain process is involved converting propylene oxide to propanal.

TABLE OF CONTENTS

		Page
I.	Acknowledgements	ii
II.	Abstract	iii
III.	Table of Contents	iv
IV.	Introduction	1
V.	Photoionization Ion Cyclotron Resonance Spectroscopy	
	Introduction	6
	Comparison of Electron Impact and Photoionization ICR	9
	Experimental--Argon Resonance Line Lamps	16
	Experimental--Photolysis Analysis	26
VI.	Photoionization Study of Three C_3H_6O Isomers	
	Introduction	28
	Experimental	30
	Results and Discussion	
	(i) Propanal	35
	(ii) Acetone	35
	(iii) Propylene Oxide	39
VII.	Calculation of Power Absorption in Photoionization ICR	
	Ion Production and Concentration	45
	Power Absorption and Signal Intensity	50
	Lineshape in the Case of a Non-Reactive Primary Ion	55
VIII.	References	59

INTRODUCTION

Ion cyclotron resonance (icr) spectroscopy is a relatively new (1) mass spectrometric tool with a number of advantages for studying gas phase ion chemistry, especially in the determination of reaction sequences. The cyclotron motion of a charged particle in a uniform magnetic field is used in determining the mass to charge ratio, m/e, of ions in the icr spectrometer. A variety of factors makes it convenient to study ion molecule reactions in the pressure range 10^{-8} to 10^{-3} torr, the long path length of ions in the cell allowing third and fourth generation product ions to be detected at the higher pressures. The low pressure limit is set by the sensitivity of the detection system, while the upper limit of useful pressure is set by the resolution, which varies inversely with pressure (2). Unlike most other mass spectrometers, ions are detected in the same region and at the same time as they are reacting, rather than being withdrawn from a reaction chamber and accelerated to a detector.

The icr cell is pictured schematically in Figure 1. An electromagnet produces a uniform magnetic field $\underset{\sim}{H}$ in the -z direction. Charged particles in this field move in circular orbits in the x,y plane with cyclotron frequency $\omega_c = qH/mc$ (Gaussian units), where c is the speed of light. The motion of ions in the z-direction is limited by static potentials applied to the trapping plates; a positive potential on both plates will force positive ions to oscillate between the plates (3). Besides the trapping field in the z-direction, there are drift plates on the top and bottom of the cell to which an electric field $\underset{\sim}{E}$ can be

Figure 1 Cutaway view of the ion cyclotron resonance spectrometer cell. As described in the Introduction, the square wave generator attached to one trapping plate is replaced by a static potential $+V_t$ for positive ions. The use of the square wave generator is described on pages 21 and 24.

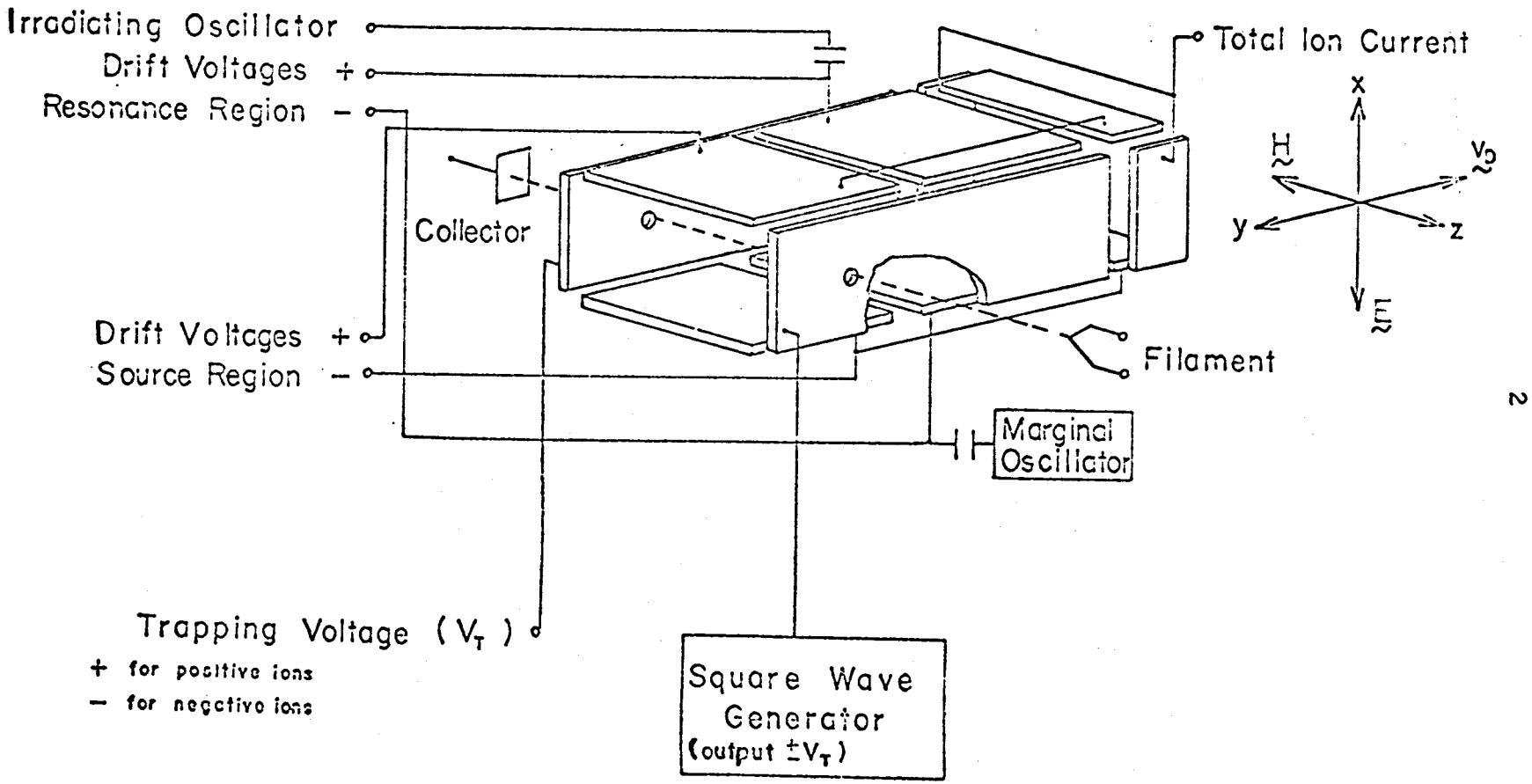
Irradiating Oscillator
Drift Voltages +
Resonance Region −
Collector
Total Ion Current
Drift Voltages +
Source Region −
Filament
Marginal Oscillator
Trapping Voltage (V_T)
+ for positive ions
− for negative ions
Square Wave Generator
(output $\pm V_T$)
x
y
z
H_z
V_D
E_y

applied in the -x direction. Normally, the drift field moves ions formed at the electron beam into the resonance region, where they are detected. The equation of motion of a charged particle in the presence of magnetic and electric fields, without considering collisions with other particles, is

$$m\, d\underset{\sim}{v}/dt = q\,\underset{\sim}{E} + q\,\underset{\sim}{v} \times \underset{\sim}{H}/c.$$

Considering only the drift and magnetic fields, where $\underset{\sim}{E} = -E\underset{\sim}{i}$ and $\underset{\sim}{H} = -H\underset{\sim}{k}$, the Lorentz force can be written in component form:

$$dv_x/dt = -\omega_c cE/H - \omega_c v_y$$

$$dv_y/dt = \omega_c v_x$$

$$dv_z/dt = 0.$$

A general solution to these equations is

$$v_x = \sin \omega_c t$$

$$v_y = -\cos \omega_c t - cE/H,$$

which is circular motion in the x,y-plane superimposed on a constant drift velocity $v_d = cE/H$ in the -y direction. Note that this velocity is independent of the charge and mass of the ion. The motion in the z-direction is not affected by the magnetic field or drift potentials.

The actual equation of motion of an ion in the icr cell includes terms expressing the effect of both reactive and non-reactive collisions with other molecules (2,4-6). However, at low pressures, where the time between collisions is comparable to the time an ion spends in the cell, the effect of collisions can be ignored. This simplified treatment is reasonably good even when product ions are detected, although collisions between ions and molecules must be occurring.

The standard ionization process is electron impact at moderate electron energies (10 to 70 eV). The electron beam crosses the source region parallel to the magnetic field. After formation, ions are drifted down the cell by the drift potentials. In the resonance region, which has drift plates electrically insulated from the drift plates in the source region, there is an rf electric field, $E_1 \sin \omega_1 t$, added to the drift potential, perpendicular to the magnetic field. The rf electric field can be considered as the sum of two contrarotating vectors; only that part which rotates in the same direction as the ion can transfer energy to the ion, in the x,y-plane. When the frequency of the rf electric field is the same as the cyclotron frequency of an ion, the ion will absorb energy from the field. Solving the equation of motion for the case of a uniform magnetic field and an rf electric field at the cyclotron frequency of the ion leads to an ion energy in the x,y-plane dependent on the time t the ion has been at resonance (4):

$$T(\omega_c,t) = \tfrac{1}{2} m (v_x^2 + v_y^2) = q^2 E_1^2 t^2/8m \qquad \text{(averaged)}.$$

The power absorption of an ion is the time rate of change of the ion energy:

$$A(\omega_c,t) = dT(\omega_c,t)/dt = q^2 E_1^2 t/4m.$$

The energy absorption is detected as a change in the Q of an L-C circuit (4). Some form of modulation, to reference the power absorption at resonance to the negligible power absorption off resonance, or when no ions are present, is used. The detector output is passed through a phase sensitive detector to recover the desired signal. The magnetic field, drift velocity, electron energy, and trapping potential can be modulated to produce a phase dependent signal (7).

Most ion-molecule reactions have cross sections that vary with the relative kinetic energy of the two reactant species. It is possible to increase the kinetic energy of an ion in the source or resonance region by subjecting it to an rf electric field at its cyclotron frequency. The power absorption in the detector circuit of a product ion which results from a reaction of the heated ion will probably be altered, due to a change in the number density of the product ion. If the power absorption of a product ion is continuously monitored in the resonance region, while a second rf electric field in the source or resonance region is swept through the cyclotron frequencies of possible reactant ions, a change in product ion signal intensity may be seen when the cyclotron frequency of a precursor ion is excited. This double resonance experiment usually allows the ionic species coupled by reaction to be unambiguously determined.

PHOTOIONIZATION ION CYCLOTRON RESONANCE SPECTROSCOPY

Introduction

In normal icr operation, ions are generated by electron impact. A beam of electrons is emitted from a hot filament wire, accelerated by a potential difference between the filament and the source region trapping plate, and collected on a plate just beyond the opposite trapping plate. The electron beam is collimated by the magnetic field as it passes through the cell. The emitted electron current, i_e, and the ion current, i_c, are related, in a one component gas at low pressure, by the expression

$$i_c \cong i_e n Q l,$$

where n is the number density of neutrals, Q is the total electron impact ionization cross section, and l is the path length of the electrons across the cell. Q varies typically from 1 to 30 x 10^{-16} cm^2 (8), i_e is regulated from 10^{-9} to 10^{-5} amps, and i_c is normally found to be from 1 to 300 x 10^{-13} amps. The usefulness of this relationship depends on the efficiency of the ion and electron beam collectors. The alignment of the electron beam and its collimation, and the proper match of drift potentials in the source and resonance regions, determines the accuracy with which the currents are measured. A practical difficulty is that the drift and trapping voltages that produce the best signal intensities do not normally permit the total ion current to be measured at the ion collector. Balanced drift voltages and high trapping voltages are usually necessary to measure the actual ion current.

A second scheme for the generation of ions uses 8 eV or higher energy photons in the vacuum ultraviolet. In this case, a suitable photon source is connected to the icr spectrometer by a window at the resonance region end of the cell casing, as indicated by the modifications shown in Figure 2. The photon beam passes down the entire cell in the y-direction, finally striking the cell casing in the area of the electrical feedthroughs.

A collimated ray of photons travelling down the cell should obey Beer's law:

$$I(x) = I_o \, e^{-\sigma n x},$$

where $I(x)$ is the photon flux at a distance x from the window, I_o is the light intensity just inside the window, and σ is the total absorption cross section of the gas in the cell. Assuming that the drift and trapping fields do not extend appreciably beyond the limits of the cell plates, only ions formed between the cell plates can later be trapped by the ion collector. Applying normal drift and trapping voltages to the source and resonance regions, the ion current detected should be

$$I_c = \eta \, I_o \, (e^{-\sigma n d_s} - e^{-\sigma n d_c}) \text{ ions/sec},$$

where η = ionization yield, or the probability that excitation by a photon will produce ionization. Both σ and η are energy dependent (9). η is generally less than one for polyatomic molecules, and typically ranges from 0.2 to 0.7 (9,10). For acetone at the region of the argon resonance line lamp to be discussed later, 11.6 - 11.8 eV, σ is roughly 0.5 Å^2 (11).

Figure 2 Modifications of the standard icr cell for photoionization studies. (a) Schematic diagram of the cell and interface with the lamp, viewed in the x direction. The interface connects to the lamp and flange with O-ring seals; a pressure of roughly 5 microns is maintained in the interface by a small roughing pump. (b) Diagram defining distances in the cell. Actual values are $l_r = l_s = 6.35$ cm; $l = 2.54$ cm; $l_c \cong 3.5$ cm; and $d_s \approx 15$ cm.

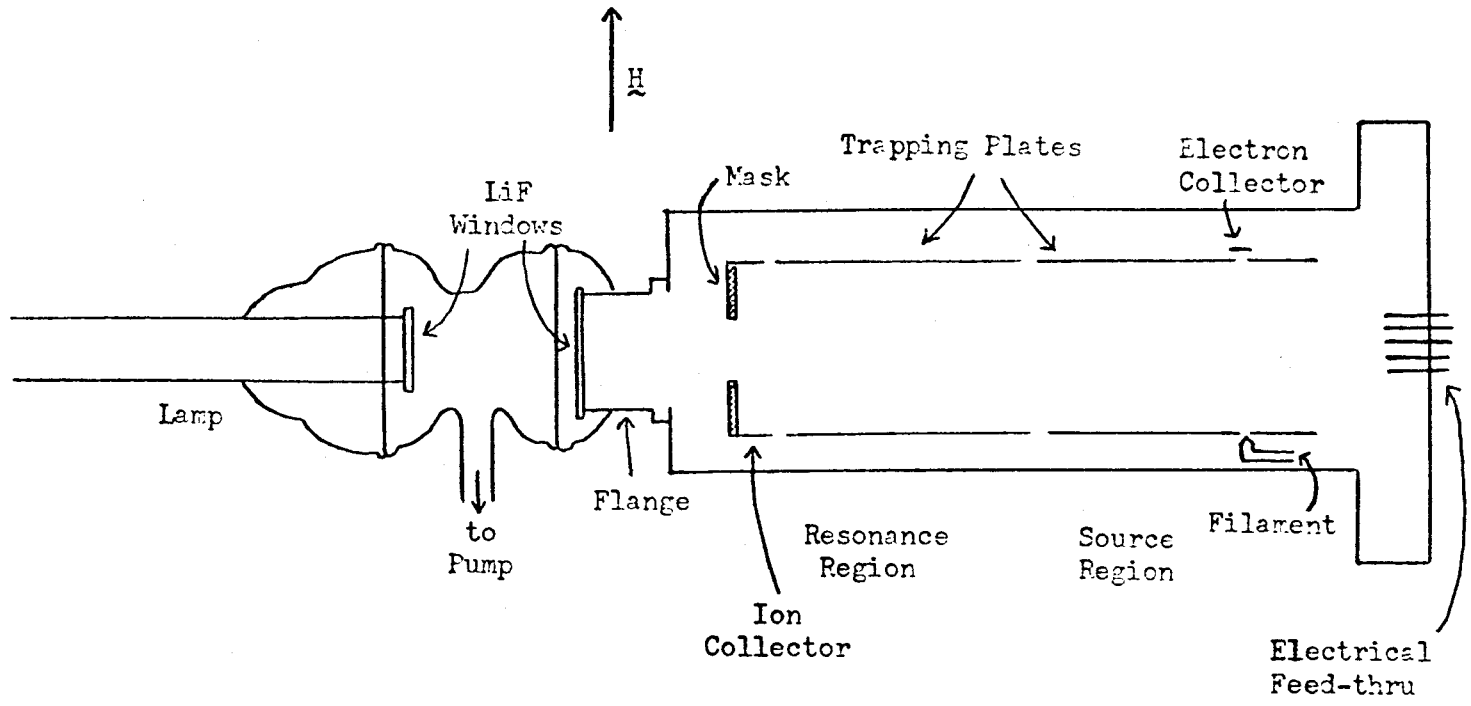
H
Trapping Plates
Electron Collector
Mask
LiF Windows
Lamp
to Pump
Flange
Resonance Region
Source Region
Filament
Ion Collector
Electrical Feed-thru

(a)

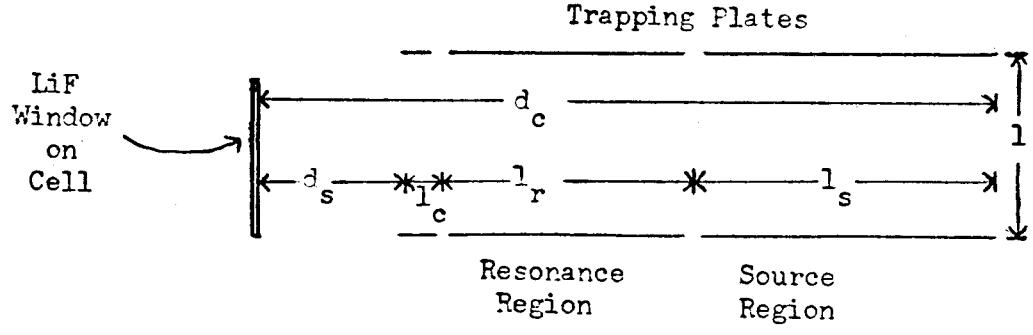
Trapping Plates
LiF Window on Cell
d_c
d_s
l_c
l_r
l_s
l
Resonance Region
Source Region

(b)

Comparison of Electron Impact and Photoionization ICR

The development of an intense light source in the vacuum ultraviolet allows the many advantages of the ion cyclotron resonance spectrometer discovered in electron impact ionization studies to be applied to photoionization experiments as well. A number of differences in the two methods will be examined below.

(i) Energy Resolution

It is simple to produce a fairly intense electron beam from a heated wire, and to generate any desired energy by using suitable electric fields. The beam current can be used to maintain a constant electron flux through feedback circuits. However, because electrons are emitted from the filament with different energies and initial directions, the electron beam that enters the source region will have a slight energy spread. The trapping and drift potentials applied in the source region produce a potential well in the center of the cell (3), which causes the electron energy to vary as an electron crosses the cell. This leads to an energy spread of the order of 0.3 eV about the nominal electron energy (12). Absolute measurements of the electron energy are difficult, so indirect and possibly inaccurate methods are used in electron impact experiments.

In photoionization icr, the energy and propagation direction of photons that enter the cell are not affected by the magnetic and electric fields present. In the case of resonance line lamps as used in this study, radiation of known energy and small bandwidth can be obtained from the emission lines of the gas used. The rare gas and hydrogen lamps

normally used produce either one or two intense lines, as listed in Table I. The argon resonance lines (11.62 and 11.83 eV) are the most energetic that can be passed through crystal windows (LiF) (13) and are therefore the most often used for photoionization work, although they do have an energy difference of 0.21 eV. Using a lithium flouride window, the intensity of the more energetic 1048.2 Å line varies from about 20% to 100% of the 1066.7 Å line after passing through the window, depending on the operating conditions.

A variety of continuum sources are also available (13), which could be coupled with a monochromator to supply nearly mono-energetic photons. Besides being more cumbersome than the resonance line lamps, the continuum/monochromator source would suffer from decreased photon fluxes. Argon resonance line lamps with photon fluxes of 10^{12} to 10^{14} photons/sec can readily be made (14,15), the intensity being inversely related to the useful life of the lamp. Continuum sources with an output of 10^{8} to 10^{9} photons/sec/Å have been made (16); however, to generate sufficient ions for operating the icr spectrometer would mean bandwidths of 100 Å or more at lower pressures, which would give a photon energy spread of the order of 1 eV.

(ii) Sample Pyrolysis

The presence of a hot filament in the cell casing during electron impact icr can lead to pyrolysis of the gas being studied. The filament typically operates at 1500 °K (17). When working at pressures above 10^{-4} torr, the VacIon pump that pumps continuously on the spectrometer cell must be partially throttled off to avoid overloading it; contamination of the sample gas with pyrolysis products will be especially likely

Table I

Lowest Resonance Emissions and Ionization Potentials of the Rare Gases and Hydrogen (Data from Reference 13)

Gas	Resonance Emission (Å)	(eV)	Ionization Potential (Å)	(eV)
He	584.3	21.22	504.3	24.59
Ne	735.9*	16.85*	574.9	21.56
	743.7	16.67		
Ar	1048.2*	11.83*	786.9	15.76
	1066.7	11.62		
Kr	1164.9	10.64	885.6	14.00
	1235.8*	10.03*		
Xe	1295.6	9.57	1022.1	12.13
	1469.6*	8.44*		
H	1215.7	10.12	911.6	13.60

* Wavelength of the strongest emission.

at these higher pressures. As an example of the difficulties possible if the pump is completely throttled off, the pressure doubled in about $2\frac{1}{2}$ seconds with silane at a pressure of 2×10^{-4} torr, using 70 eV electron energy. The pressure doubling was accompanied by a marked decrease in the largest peak, SiH_3^+, and an increase in the H_3^+ peak (18). This was attributed to the decomposition of SiH_4 to Si and H_2 on the hot filament, the hydrogen then being ionized and reacting to produce H_3^+. Although cases have not been well documented, similar problems can be expected with many organic molecules at pressures above 10^{-4} torr. Of course, pyrolysis cannot occur with a photon source located outside the cell casing as in photoionization icr.

(iii) Space Charge Effects

The electron beam crossing the source region sets up an electric and magnetic field in its vicinity, thus affecting the motion of ions and electrons in the region of the electron beam. Beauchamp (4) reports that the magnetic field caused by the electron beam is too small to have any affect, but that the space charge depression ΔV of the potential at the electron beam may be. Calculations show that (4)

$$\Delta V = 7.6 \times 10^5 \, i_e/\sqrt{V_o} \text{ volts},$$

where V_o is the nominal electron energy in eV. This sets up an electric field of approximately $2\Delta V/d$, where d is the spacing between the drift plates, and can present problems when it is comparable to the drift field, V_s/d, set up by the drift potential in the source region. For an emission current of 6 μamp and an electron energy of 14 eV, the space charge depression is $\Delta V = 1.2$ volts; normal drift potentials are from

0.2 to 1.6 volts. This space charge depression also contributes to the spread in electron energies as the electron beam crosses the cell. To avoid the effects of the space charge depression on the resonant cyclotron frequency of ions, the resonance region is physically separated from the electron beam. In photoionization icr experiments, the space potential is not affected by the photon beam in the cell.

(iv) Electron Beam and Photon Current Measurement

As derived previously, there are relatively simple expressions relating the ion and electron currents in the case of electron impact ionization and the light intensity and ion current in the case of photoionization. The electron beam current is routinely measured by an electrometer in electron impact studies, and good agreement between calculated and measured pressures can be obtained using the ion and electron current relationship. In photoionization studies, it would be possible to determine the light intensity with a scintillation or photo-electron counter inside the cell, although the efficiency of the counter would need periodic checking. The light intensity just inside the cell window decreases with time, necessitating several measurements of the photon flux with no gas in the cell.

In photoionization icr, trapping voltage modulation (to be described later) with zero drift potentials is the normal mode of operation. Thus no ion current is measured at the ion collector, and making ion current measurements at the trapping plates is complicated by the modulation of the very small currents involved. Electron fluxes and ion currents, in practice, are much easier to measure than photon fluxes and the resulting ion currents.

(v) Threshold Ionization Efficiency

It has been found both experimentally (19,20) and theoretically (20,21) that at threshold the cross section for direct ionization is nearly proportional to $(E - E_o)^{n-1}$, where E_o is the threshold energy, E the energy of the ionizing particle, and n the number of electrons leaving the activated collision complex. In photoionization, where n = 1, the threshold behavior for parent ion production is nearly a step function of photon energy. In electron impact ionization, n = 2 and there is a linear increase of ion abundance with electron energy. In photoionization studies it is often possible to get exclusively parent ion at intensities great enough to be detected by the spectrometer, without having any fragment ions present. When electron impact is used, however, it is often found that by the time a useful parent ion signal is obtained, the fragment ion intensity is also significant (8,20). Thus photoionization icr may allow the study of parent ion reactions without competition from reactions of fragment ions.

(vi) Neutral Product Analysis

The techniques of photolysis analysis can be used in studying ion-molecule reactions when using a photon source. A gas sample can be photolyzed by the same lamp used in the photoionization icr experiment and analyzed by a gas chromatograph/mass spectrometer to determine the neutral products (22). The products produced by ion-molecule reactions could be identified from those produced below the ionization threshold by performing another photolysis below the ionization potential of the gas, using either a Xenon or Krypton resonance line lamp. Radical and

ion scavenging experiments may also help to determine the ion chemistry involved (23). It is extremely difficult to analyze the neutral products in electron impact studies.

Experimental--Argon Resonance Line Lamps

One basic design of resonance line lamp was used in the photoionization studies. The basic components of the lamps (15) are (i) a cylindrical tube in which a gas is excited by a microwave discharge to produce the ultraviolet radiation; (ii) a window at one end of the discharge tube to pass radiation of the desired wavelength; (iii) an access port for evacuating the lamp before filling and for introducing the desired gas; and (iv) a gettering assembly or other device to control impurities. The lamps used in these experiments are descendants of a lamp designed by Arthur Lane (14) here at Caltech. Figure 3 shows the first lamp (lamp I) used in this study, with a vacuum stopcock on the access arm and an O-ring seal on the getter side arm to permit the titanium filament to be replaced. Figure 4 shows a modified lamp (lamp II), in which the O-ring seal is removed and a glass constriction added to the access arm, so that the filled lamp has no greased components. Eliminating the stopcock grease allowed the lamp to be used for considerably longer periods before impurity lines in the spectrum became excessive.

The discarge tube is made of pyrex glass of 17 mm outside diameter and roughly 2 mm thick walls. The tube is 23 cm long in lamp I, and was lengthened to 26 cm in lamp II to keep the discharge further from the window. The discharge is normally maintained in a region about 12 cm long, and kept at least 6 cm from the window. The closer the discharge is brought to the window, the hotter the window gets; heating the lithium flouride window causes its cutoff (nominally 1040 Å at 25 °C) to shift to

Figure 3 Rare gas resonance line lamp (lamp I). The cold finger was not found to be useful with the argon lamp, and was removed during the course of the experiments.

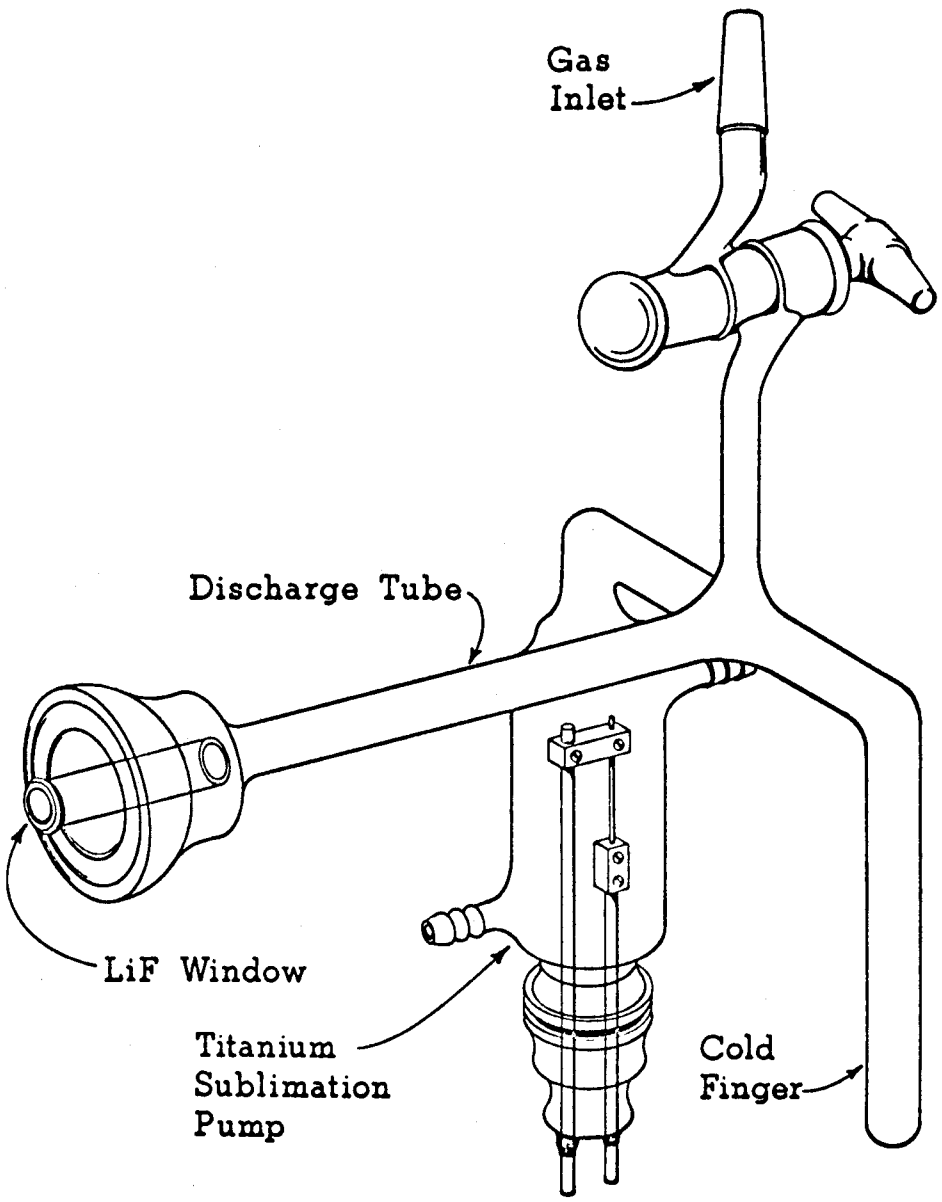
Gas
Inlet
Discharge Tube
LiF Window
Titanium
Sublimation
Pump
Cold
Finger

Figure 4 Rare gas resonance line lamp (lamp II). The sidearm on the bell near the window was added so that the interface between lamp and flange could be removed, bringing the lamp closer to the cell.

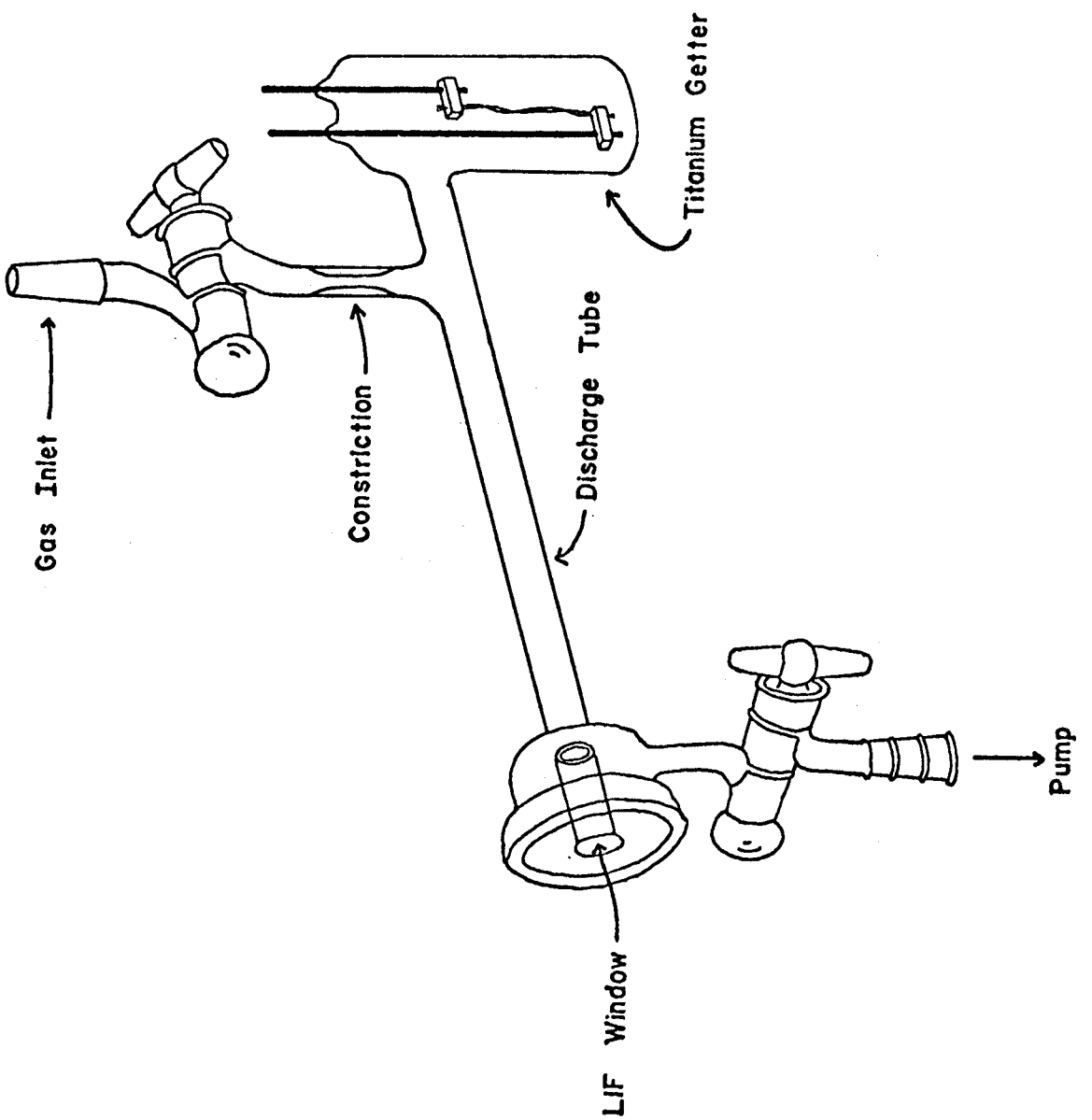
Titanium Getter
Gas Inlet
Constriction
Discharge Tube
LIF Window
Pump

longer wavelengths (24). Figure 5 shows the effect on the transmission of the 1048.2 Å line of argon of bringing the discharge right up to the window. Heating the epoxy holding the window to the glass also releases contaminants from the epoxy, shortening the useful life of the lamp.

The window is a wafer of lithium flouride crystal, approximately 1 mm in thickness and 2.5 cm in diameter. Over twenty usable windows were cleaved from a 2 inch long cylindrical LiF crystal obtained from the Harshaw Chemical Company. Cleavage was effected by razor blade, hammer, and steady hand. Through trial and error, it was found that roughly halving the crystal with each cut produced the fewest breaks, while attempting to cut a 1 mm window from one end of a large crystal nearly always caused the window to break. Torr Seal, a high vacuum epoxy made by Varian Associates, was used to cement the window to the ground glass end of the discharge tube. The window was kept under vacuum as much as possible to protect it from atmospheric moisture. The formation of F-centers (25) with use of the lamp causes the window to yellow and decreases transmission. A small mercury discharge lamp brought right up to the yellowed window was found to slowly bleach the window and improve transmission.

The getter filament consists of two 0.020 inch diameter titanium wires, 99.95% pure as obtained from Research Organic/Inorganic Chemicals Company, wound around a 0.02 inch diameter tungsten support wire. In the lamp I design, the getter assembly can be easily removed by the O-ring seal and the filament changed as needed. With lamp II, changing the getter wires required cutting the glass envelope of the getter, but a leak-proof seal was made by the annealed glass wall. A special

Figure 5 Behavior of the emission of the argon resonance line lamp for two positions of the discharge relative to the window. Lamp I was used, with only the one window on the lamp in the photon path.

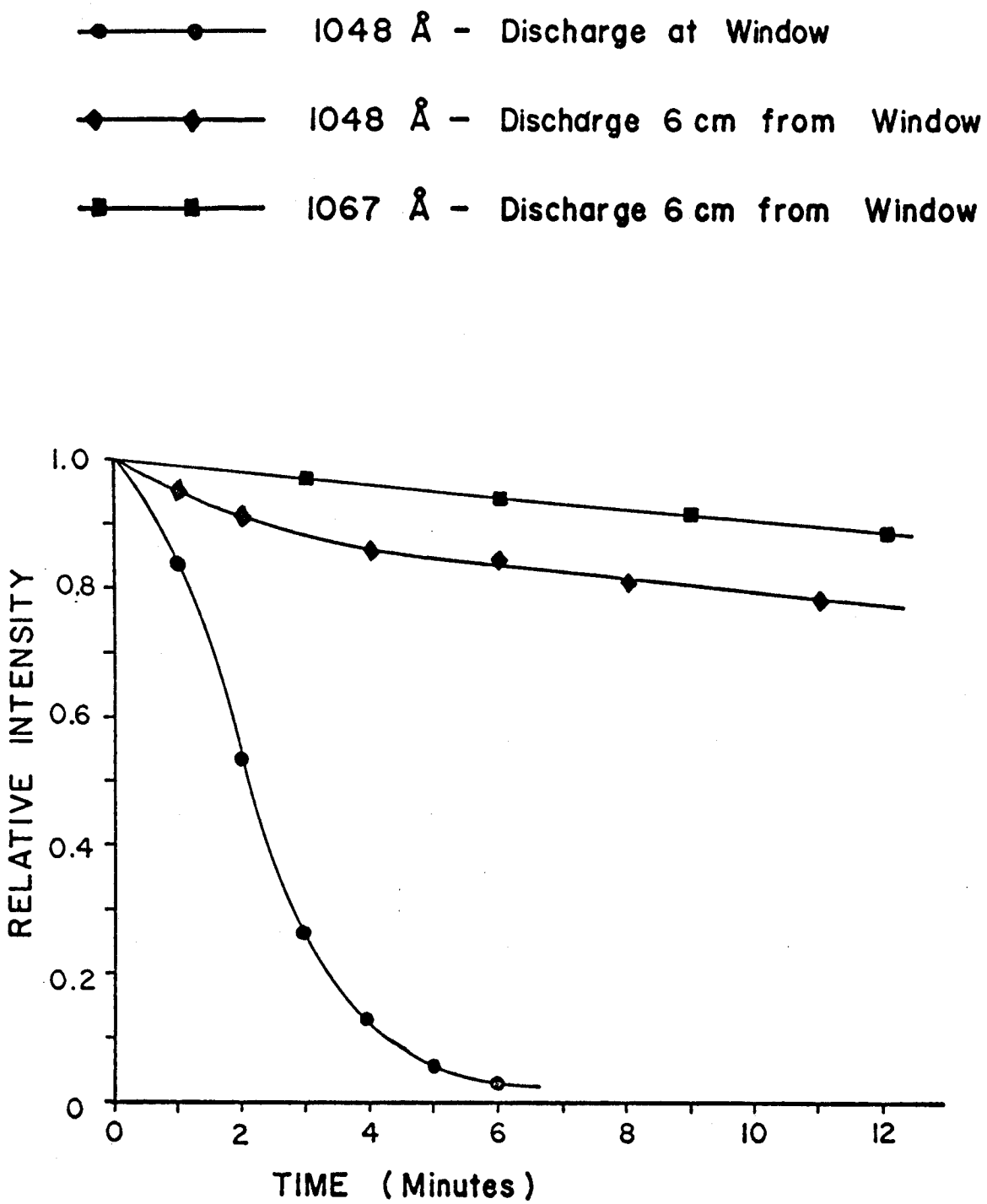
1048 Å - Discharge at Window
1048 Å - Discharge 6 cm from Window
1067 Å - Discharge 6 cm from Window
RELATIVE INTENSITY
1.0
0.8
0.6
0.4
0.2
0
0
2
4
6
8
10
12
TIME (Minutes)

vacuum line, used only for the preparation of the lamps, is shown in Figure 6. Before filling, the lamp was pumped to 4×10^{-7} torr or lower with the oil diffusion pump. The titanium was deposited on the inside glass walls of the getter by passing 19 amps at six volts through the filament for approximately thirty minutes, after degassing for a similar period. Two or three mirror coatings could usually be deposited before the filament wires broke. The lamp was then filled with Airco research grade argon to a pressure of several tenths of a torr. The pressure of argon added to the lamp was measured by a Veeco DV-1M thermocouple gauge. The conversion between air and argon pressure readings was made using expansion from a known pressure read by a Wallace-Tiernan gauge.

The resonance line discharge was maintained by a Raytheon microwave power generator, 85 watts at 100% power, which operates at 2450 ± 25 MHz. The discharge was initiated by a spark from a Tesla coil. The simple V-shaped antenna was positioned from 1 to 5 cm from the discharge tube.

The output of the lamps was recorded with a McPherson half meter vacuum monochromator, Seya-Namioka type, with a 1200 lines/mm grating. A layer of sodium salicylate was used as a constant quantum efficiency scintillator (26), with an EMI 9514S photomultiplier tube used to read the photon current. The sodium salicylate was deposited in the manner described by Knapp (27) to a density of roughly 3 mg/cm^2, eight months before the first spectra here reported were recorded. Figure 7 shows the instrumental set up for recording the spectra of the lamps.

The photon beam is left on continuously in photoionization icr, and thus ions are formed continuously throughout the cell. The ion

Figure 6 Vacuum line designed for preparation of rare gas resonance line lamps. A base pressure of 1×10^{-7} torr is obtained in the manifold, which is never exposed to air.

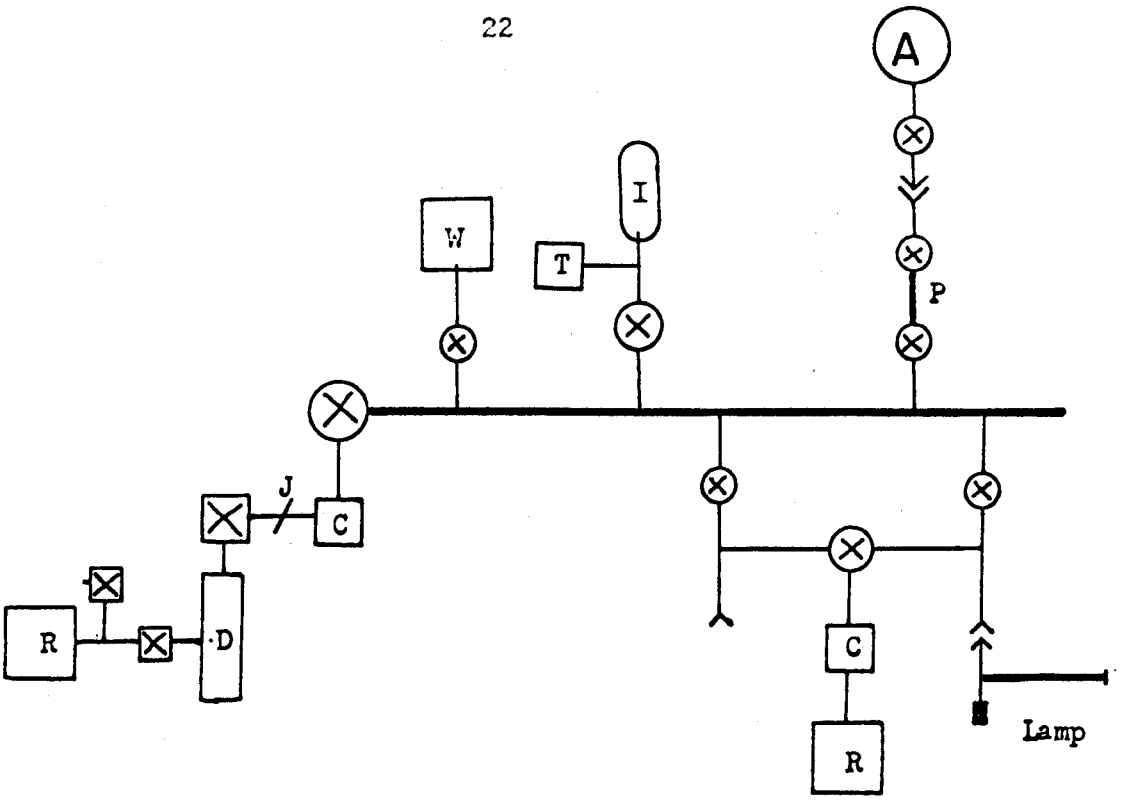

A — Argon Reservoir

C — Cold Trap

D — Diffusion Pump

I — Ionization Gauge

P — Gas Pipette

R — Roughing Pump

T — Thermocouple Gauge

Brass Valves

Vacuum Stopcocks

W — Wallace-Tiernan Gauge

The vacuum line is all metal to the left of joint J, all glass to the right of joint J.

Figure 7 Experimental set up used to monitor the output of the resonance line lamps. The photolysis cell can be mounted between the lamp and the entrance slit of the monochromator to record the output of the lamp prior to photolysis.

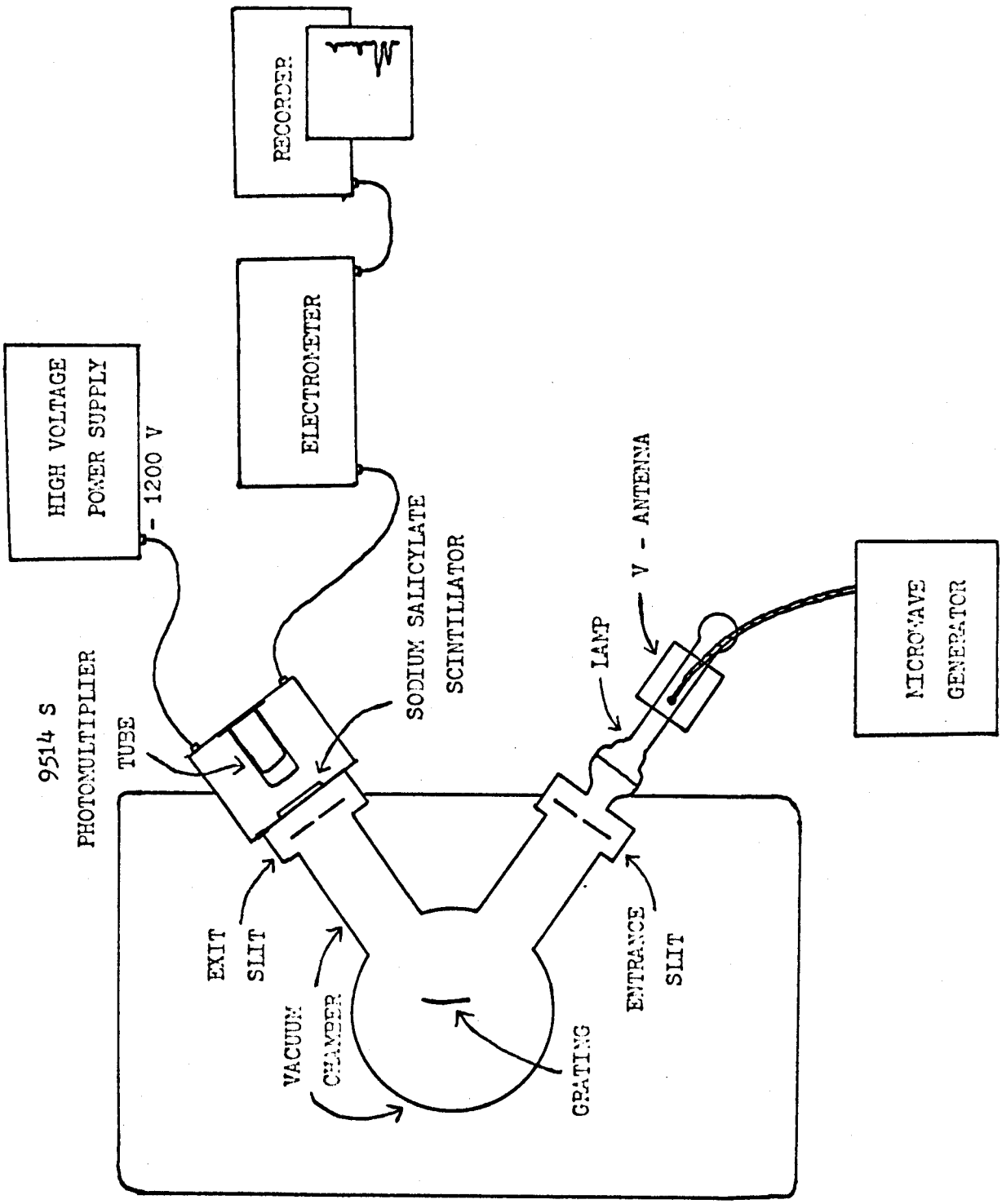
RECORDER
ELECTROMETER
HIGH VOLTAGE
POWER SUPPLY
- 1200 V
9514 S
PHOTOMULTIPLIER
TUBE
SODIUM SALICYLATE
SCINTILLATOR
LAMP
V - ANTENNA
MICROWAVE
GENERATOR
EXIT
SLIT
VACUUM
CHAMBER
GRATING
ENTRANCE
SLIT

concentration is limited, and the detector signal modulated, by trapping voltage modulation. The potential applied to one trappping plate in the source and resonance regions is held at a constant $+V_t$ volts, while on the other side, the trapping potential varies in a square wave from $+V_t$ to $-V_t$ volts. Positive ions are trapped when both trapping plates are at $+V_t$; they are swept to the negative plate and neutralized when the potential on that plate switches to $-V_t$. (Refer to Figure 1 for the electrical connections in trapping voltage modulation.) The ion concentration during the half period when ions are swept from the cell is too low to be detected by the marginal oscillator.

The lamp used in the ion cyclotron resonance studies, lamp I, was filled with 0.43 torr argon for the propanal and propylene oxide studies, and to 0.52 torr for acetone. The lamp was checked on the monochromator before and after each compound was studied; Figure 8 shows the emission after the propanal study. The relative transmission properties of the LiF windows at 1048.2 Å and 1066.7 Å (argon) and at 1215.7 Å (hydrogen) were not measured for any of the windows used, but the cutoff for LiF has been reported elsewhere (24) at about 1040 Å at room temperature. Thus each successive window the photon beam encounters enhances the higher wavelength, impurity lines relative to the argon lines, and the light that enters the icr cell will have larger impurities than indicated by the emission spectra taken separately.

Figure 8 The emission spectrum of the argon resonance line lamp (lamp I) after the propanal study. The titanium getter is in use, and the lamp is connected directly to the monochromator. The two peaks at about 2100 Å are believed to be second order diffractions of the argon peaks.

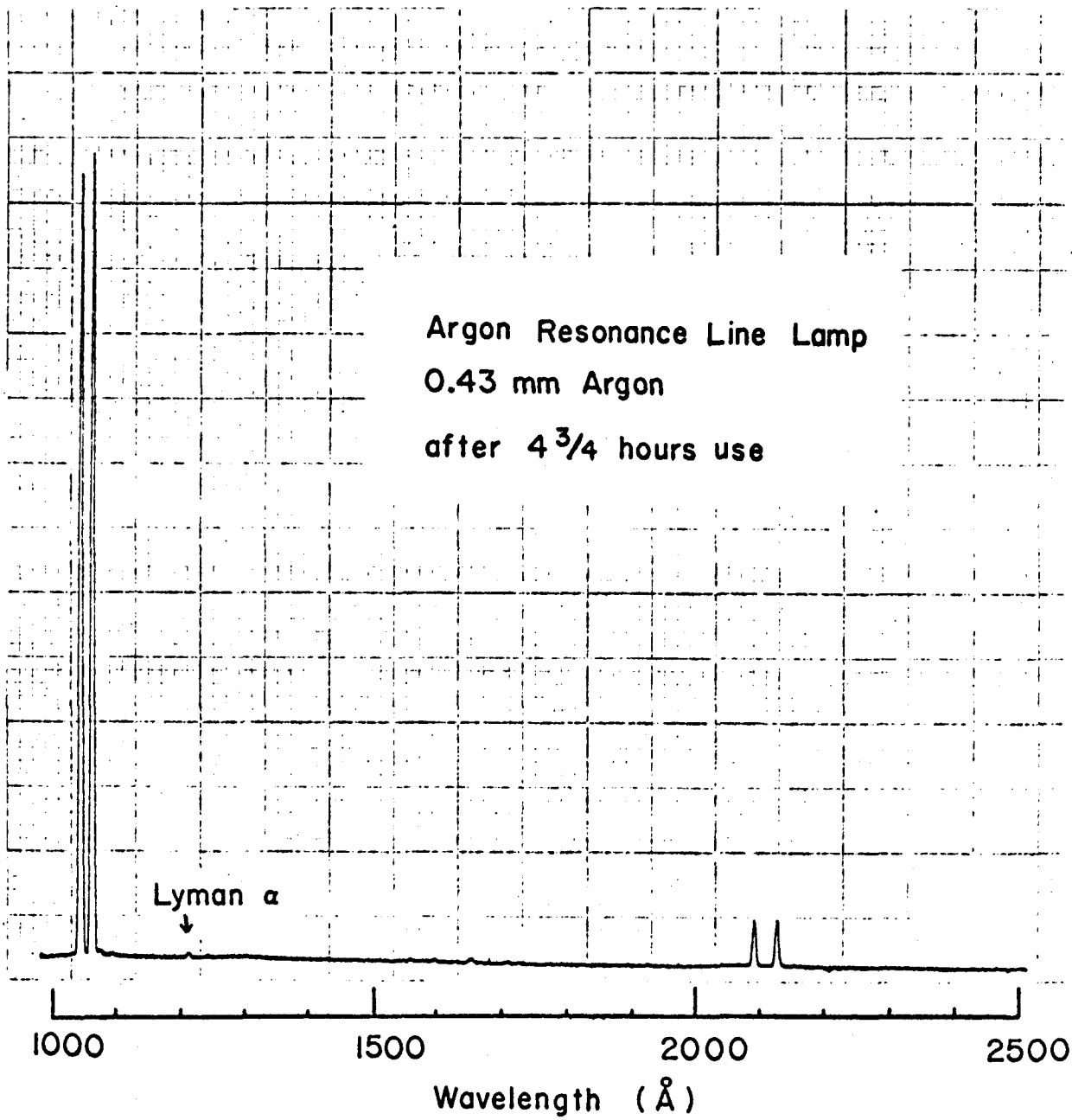
Argon Resonance Line Lamp
0.43 mm Argon
after 4 3/4 hours use
Lyman α
1000
1500
2000
2500
Wavelength (Å)

Experimental--Photolysis Analysis

One of the major advantages of photoionization mass spectroscopy is that the neutral products of ion-molecule reactions can be determined by normal photolysis analysis methods. In the present study, photolysis of propylene oxide was used to help determine the ion chemistry of the parent ion.

The photolysis cell is a pyrex vessel with two chambers, illustrated in Figure 9. The actual photolysis region is cylindrical, 2.5 cm in diameter by 12.5 cm in length, with an internal volume of 52 cm^3. At each end of the cell a 1 mm thick LiF window is mounted with Torr Seal. A vacuum stopcock is attached to the center of the cell for filling it and extracting photolysis products. Attached to the photolysis through another vacuum stopcock is a spherical ballast volume, 6.5 cm diameter, which serves as a blank.

Analysis of the products is performed using a gas chromatograph/ mass spectrometer combination. The photolysis cell is mounted on a gas inlet system of the gas chromatograph and the condensable gases (at liquid nitrogen temperatures) collected in a 9 cm long capillary U tube. The sample is allowed to come to room temperature before injecting it into a Hewlett Packard dual column gas chromatograph. The sample can be sent either to a flame ionization detector for more sensitive detection, or through a thermal conductivity detector and then to an EAI quadropole mass spectrometer, for mass analysis.

Figure 9 The photolysis cell used in the photolysis study of propylene oxide.

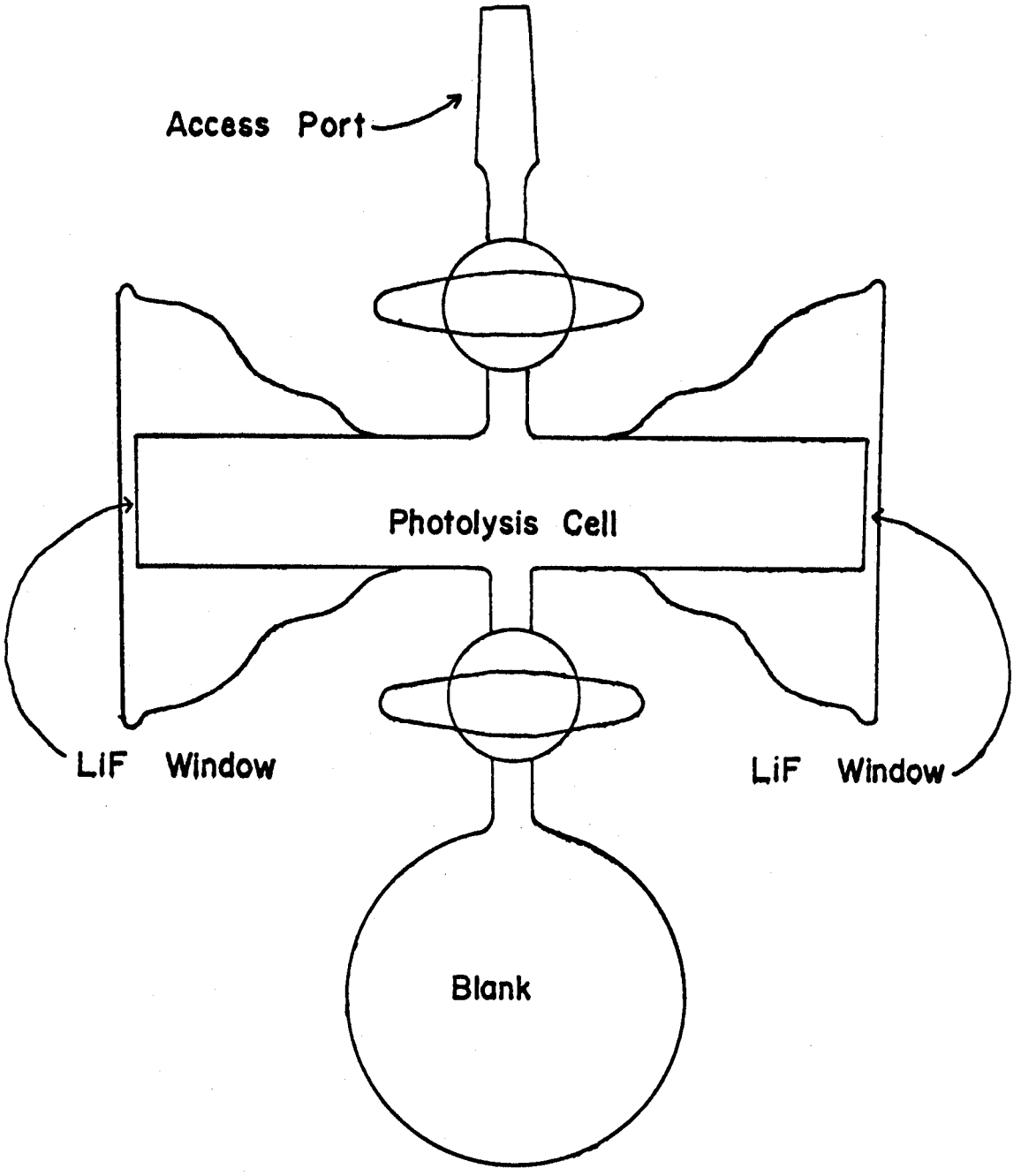
Access Port
Photolysis Cell
LiF Window
LiF Window
Blank

PHOTOIONIZATION STUDY OF THREE C_3H_6O ISOMERS

Introduction

Ion cyclotron resonance spectroscopy has been used recently to identify the structural isomers of a number of compounds (28,29), using 15 - 70 eV electron energy. Using the argon resonance line lamp described in the previous sections, a photon source with two prominent lines (11.62 and 11.83 eV) is available to perform similar studies. A preliminary study of three of the structural isomers of C_3H_6O is here reported.

There are seven chemically stable structural isomers with the empirical formula C_3H_6O, as summarized in Table II. At least six of these neutral molecules can be ionized by the argon lamp. The heats of formation of parent ions have been calculated from the ionization potentials (30); however, the structure of the parent ions is not necessarily known, especially when considerable excess energy is available in the ionizing particle.

Table II

Heats of Formation and Ionization Potentials of C_3H_6O Neutrals and Ions (Data from Reference 30)

M		$\Delta H_f^{298}(M)$ (kcal/mole)	$\Delta H_f^{298}(M^+)$ (kcal/mole)	I.P.(M) (eV)
Acetone	$CH_3\overset{\overset{O}{\|}}{C}CH_3$	-51.8	171	9.68±.03
Propanal	CH_3CH_2CHO	-48.7	181	9.98±.01
Allyl Alcohol	$CH_2=CHCH_2OH$	-32.3	191	9.67±.05
Vinyl Methyl Ether	$CH_2=CH-O-CH_3$	-27.7	178	8.93±.02
Cyclopropanol	$CH_2\overset{CH_2}{-}CH-OH$	-27*	-	-
Trimethylene Oxide	$CH_2\overset{CH_2-O}{-}CH_2$	-24	199	9.67±.02
Propylene Oxide	$CH_2\overset{O}{-}CH-CH_3$	-22	214	10.22±.02

*Calculated by group equivalent method (Reference 31).

Experimental

The present study concerns acetone, propylene oxide, and propanal. Samples were prepared from spectroscopically pure chemicals supplied by Matheson, Coleman, and Bell, and were degased on a vacuum line by repeated freezing, pumping, and thawing. Propylene oxide was examined by gas chromatography and no impurity peaks noted.

The argon resonance line lamp was connected by an evacuable interface with an O-ring joint on a flange at one end of the icr cell casing. (See Figure 2). A lithium flouride window was attached to the flange, so that the cell casing was vacuum tight. The photon beam is collimated by a mask on the ion collector end of the icr cell. The opening in the mask is 13 x 9 cm.

Trapping voltage modulation was used with one trapping plate held at a constant $+V_t$ and the opposite plate varied from $+V_t$ to $-V_t$ in a square wave. At low modulation frequencies, ions at resonance will absorb enough energy so that they spiral out and strike the top or bottom drift plates and are neutralized. Observing the output of the detector on an oscilloscope, the trapping frequency was lowered until the power absorption began to flatten out. The flattened portion of the power absorption curve represents a steady state concentration of the ion at resonance, with the rate of production equaling the rate of neutralization. A frequency of 23 hz was chosen as giving a strong signal but not allowing many ions to reach the drift plates. This corresponds to a trapping period T_o = 22 msec, or a square wave period of 44 msec. The following diagram illustrates the resonant power absorption of an ion at a very

low modulation frequency:

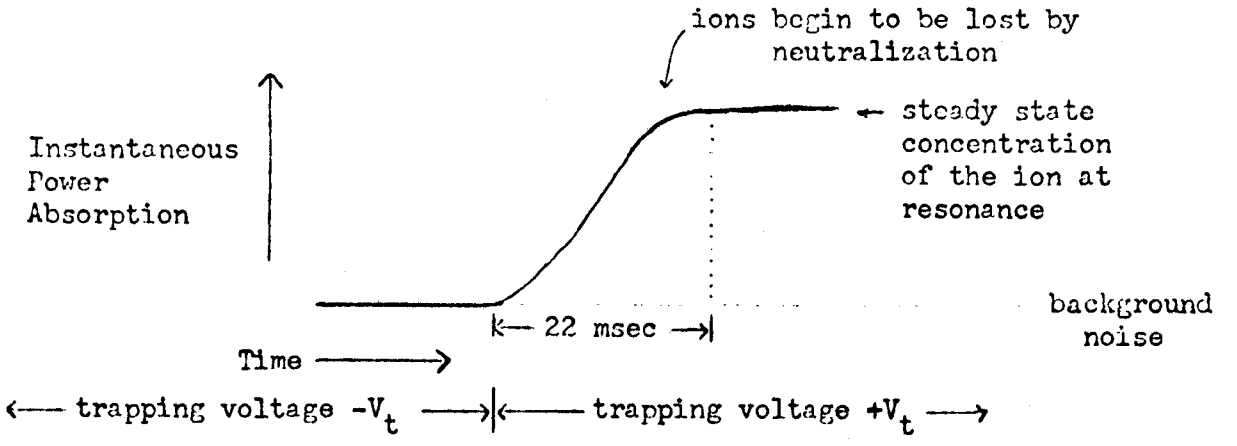

The best signal was obtained when small (0.1 - 0.3 volt) drift potentials were applied on the upper drift plate in the resonance region, with the other three drift plates at ground.

Since ions are continuously formed in the resonance region of the cell, primary ions can be detected at higher pressures in photoionization icr than is possible in normal electron impact icr. The concentration of ions in the resonance region during photoionization icr should increase linearly with time from the instant the trapping voltage becomes positive, unless the concentration of ions becomes so great that some are forced out by space charge effects. With the trapping times and photon fluxes used here, it is not expected that space charge effects will be significant.

A typical photoionization icr spectrum is shown in Figure 10, a spectrum of acetone at 4.3×10^{-5} torr. The magnetic field was swept to bring the cyclotron frequency of each ion into resonance with the fixed observing rf oscillator. At an observing frequency of 153.7 Khz,

Figure 10 Photoionization icr single resonance spectrum of acetone at 4.3×10^{-5} torr. Trapping voltage modulation was used with zero drift potentials and fixed frequency observing oscillator.

successive mass peaks are separated by 100 gauss. The spectrum shown in Figure 10 was a ten kilogauss scan made in ten minutes, covering 100 mass units. The spectra taken in the course of the pressure study were made at the rate of 1 kilogauss per 10 minutes, and only the regions where peaks were known to occur were scanned. Several full scans, as in Figure 10, were made to insure that all peaks were detected. The slower scan rate was used to get improved signal to noise ratio with a longer time constant. Pressures below 10^{-5} torr were measured by the current in the Vac Ion Pump, while above 4×10^{-5} torr a Baratron capacitance manometer was used. In the region between 1 and 4×10^{-5} torr, both pressure measurements were taken, which allowed the Vac Ion Pump pressure readings to be calibrated. The capacitance manometer was independently calibrated before this study.

Double resonance was performed during the photoionization studies, with the irradiating oscillator connected to the resonance region drift plates. Good results were obtained, limited only by the small signal intensities of some product ions. Figure 11 shows the double resonance results for acetone at 6.3×10^{-5} torr. Note that varying the irradiating frequency rather than the magnetic field produces a nonlinear mass scale.

Figure 11 Photoionization icr double resonance spectra of some product ions in acetone at 6.3×10^{-5} torr. The irradiating oscillator is connected in the resonance region of the cell.

Observe m/e 59

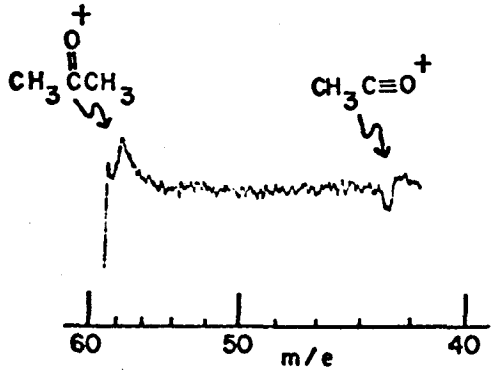

Observe m/e 101

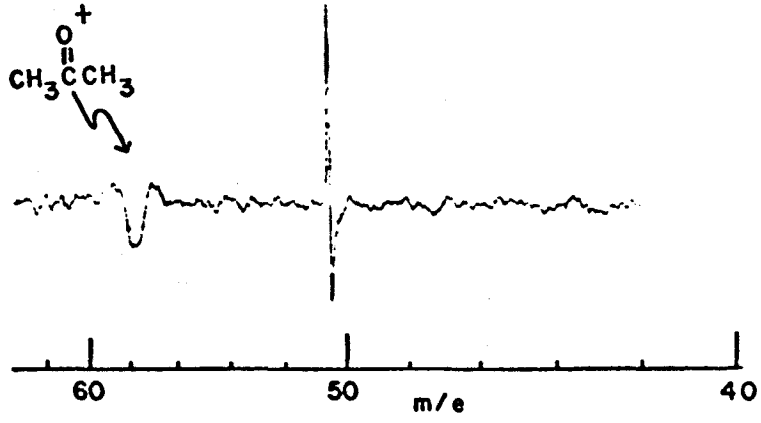

Observe m/e 117

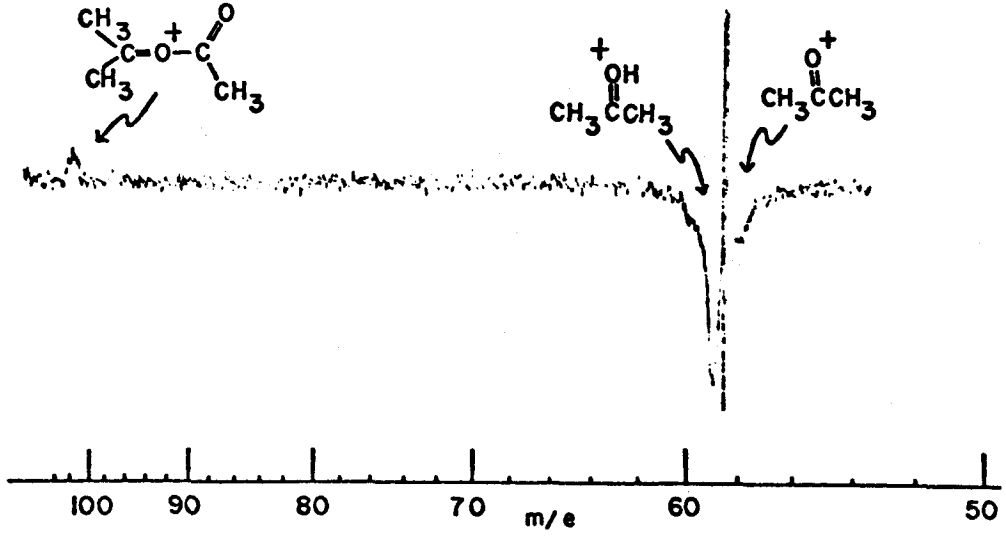

Results and Discussion

(i) Propanal

Figure 12 shows the variation in signal intensity as a function of pressure of the ions in propanal. The chemistry involved can be easily deduced from the pressure dependence of the various ions: the parent ion reacts to form the protonated parent; the protonated parent clusters with the parent neutral, which forms the proton bound dimer upon collisional stabilization. A fragment ion of mass 57 does not undergo reaction. These reactions and probable structures of the ions involved are given in Table III.

(ii) Acetone

The ion chemistry of acetone is more complicated, as indicated in the pressure plot in Figure 13. The principal reaction scheme is the same as that in propanal: parent ion reacts to form the protonated parent ion, which in turn clusters with the parent neutral to form the proton bound dimer. At the energy of the argon resonance lines, there is one fragment, accounting for roughly 18% of the initial ionization, present: $CH_3C{\equiv}O^+$ at m/e 43 (loss of methyl radical from parent ion). The fragment ion reacts by proton transfer to produce the protonated parent. The parent ion, besides reacting by hydrogen abstraction, condenses with neutral acetone to produce an ion of mass 101. The positive double resonance response from the m/e 101 ion in the spectrum of the proton bound dimer (see Figure 11) is interpreted as arising from collisionally induced decompostion of the m/e 101 ion to produce $CH_3C{\equiv}O^+$, which reacts as indicated above to produce the m/e 117 ion. The

Figure 12 Relative single resonance signal intensities as a function of pressure in propanal by photoionization icr.

Propanal (I.P. = 9.98 eV)

Argon Resonance Line Lamp $\left\{\begin{matrix} 1048.2 - 1066.7\ \text{Å} \\ 11.83 - 11.62\ \text{eV} \end{matrix}\right\}$

T_o = 22msec

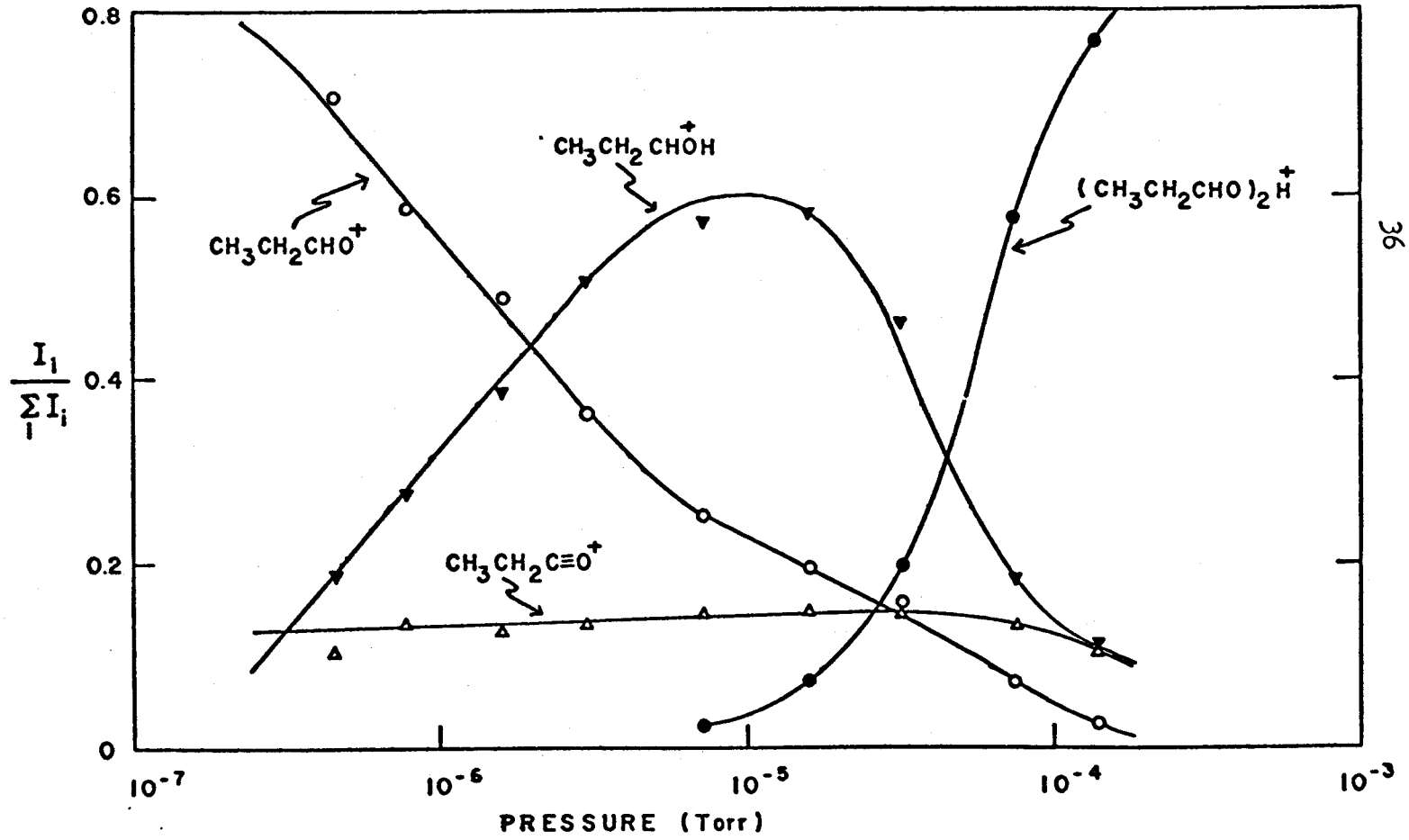

Table III Reactions of Propanal

$$\underset{(58)}{CH_3CH_2CHO^+} + CH_3CH_2CHO \longrightarrow \underset{(59)}{CH_3CH_2\overset{+}{C}HOH} + C_3H_5O \qquad (Q1)$$

$$\underset{(59)}{CH_3CH_2\overset{+}{C}HOH} + CH_3CH_2CHO \longleftrightarrow \underset{(117)}{[(CH_3CH_2CHO)_2H^+]^*} \qquad (Q2)$$

$$\underset{(117)}{[(CH_3CH_2CHO)_2H^+]^*} + CH_3CH_2CHO \longrightarrow \underset{(117)}{(CH_3CH_2CHO)_2H^+} + CH_3CH_2CHO \qquad (Q3)$$

$$\underset{(57)}{CH_3CH_2C{\equiv}O^+} + CH_3CH_2CHO \longrightarrow \text{NO REACTION} \qquad (Q4)$$

Figure 13 Relative single resonance signal intensities as a function of pressure in acetone by photoionization icr.

Acetone (I.P. = 9.68 eV)

Argon Resonance Line Lamp { 1048.2 - 1066.7 Å / 11.83 - 11.62 eV }

T_o = 22 msec

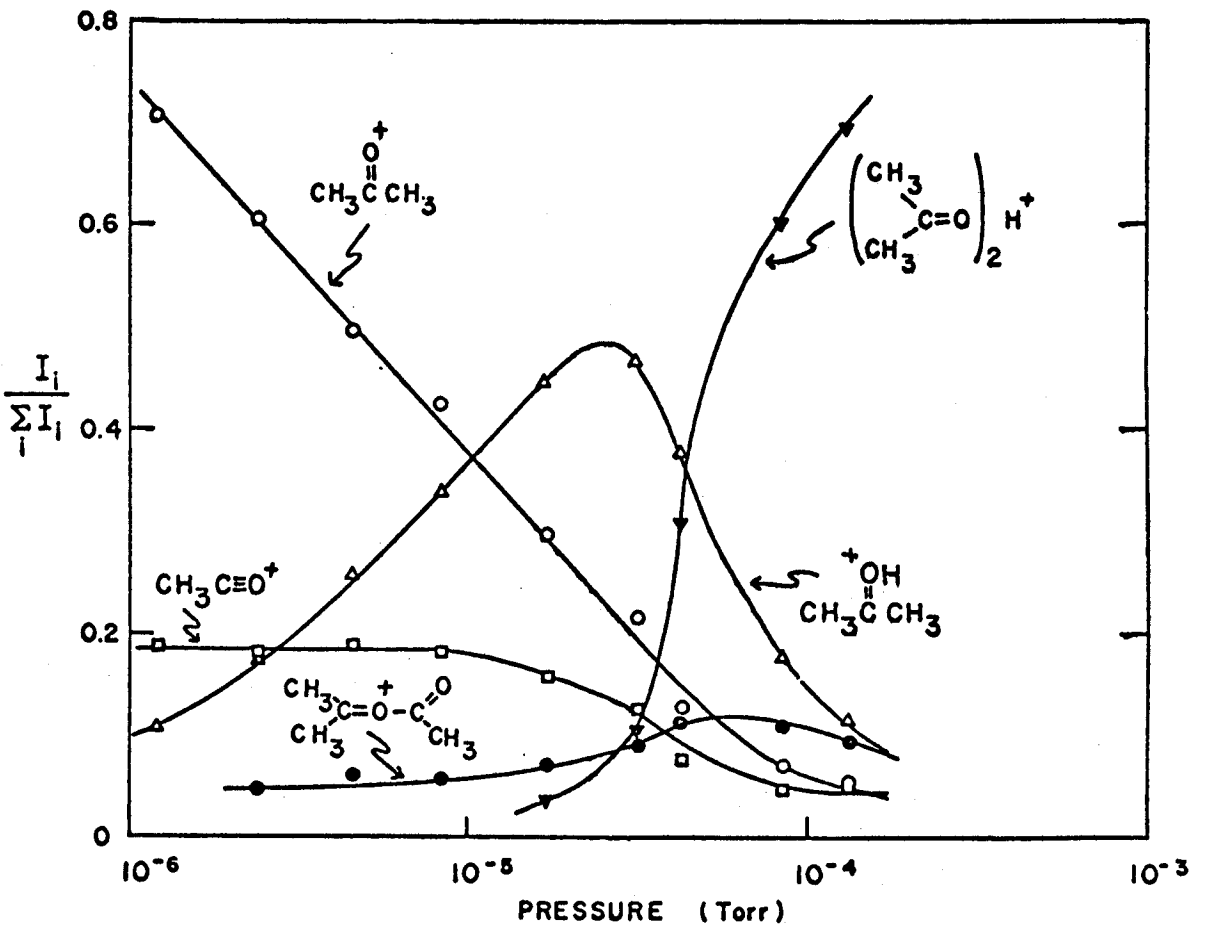

postulated reaction scheme, which agrees with a previous study (28), is listed in Table IV.

(iii) Propylene Oxide

The ion chemistry of propylene oxide is considerably different from that in acetone or propanal, as is apparent from the ion intensity data in Figure 14. The parent ion signal remains an essentially constant fraction of the total signal intensity throughout the pressure range 10^{-6} to 10^{-4} torr. The fragment ion of mass 43 (loss of methyl radical from the parent ion) is the most intense peak at low pressures. Double resonance indicates the fragment ion reacts to form the protonated parent ion of mass 59 and the ion of mass 57, loss of a hydrogen from the parent. The double resonance response for the mass 41 ion is ambiguous, but the pressure dependence indicates it also is produced by reaction of the mass 43 fragment ion. Double resonance indicates that the mass 41 ion reacts by hydride abstraction to produce the mass 57 ion. At the higher pressures, a small amount of an ion of mass 117 (the proton bound dimer?) is found, as well as an ion of mass 86, which could be either $C_5H_{10}O^+$ or $C_4H_6O_2^+$. At 10^{-4} torr, where in acetone and propanal the proton bound dimer is the major ion, in propylene oxide there is less than 2% of the proton bound dimer. This is in contrast to ethylene oxide, which has the same reaction sequence as in acetone or propanal, with the proton bound dimer the major peak at high pressures (29). The reaction sequence indicated by double resonance and the pressure dependence is given in Table V.

Propylene oxide is the least stable of the seven neutral molecules of empirical formula C_3H_6O (see Table II), and therefore could gain

Table IV Reactions of Acetone

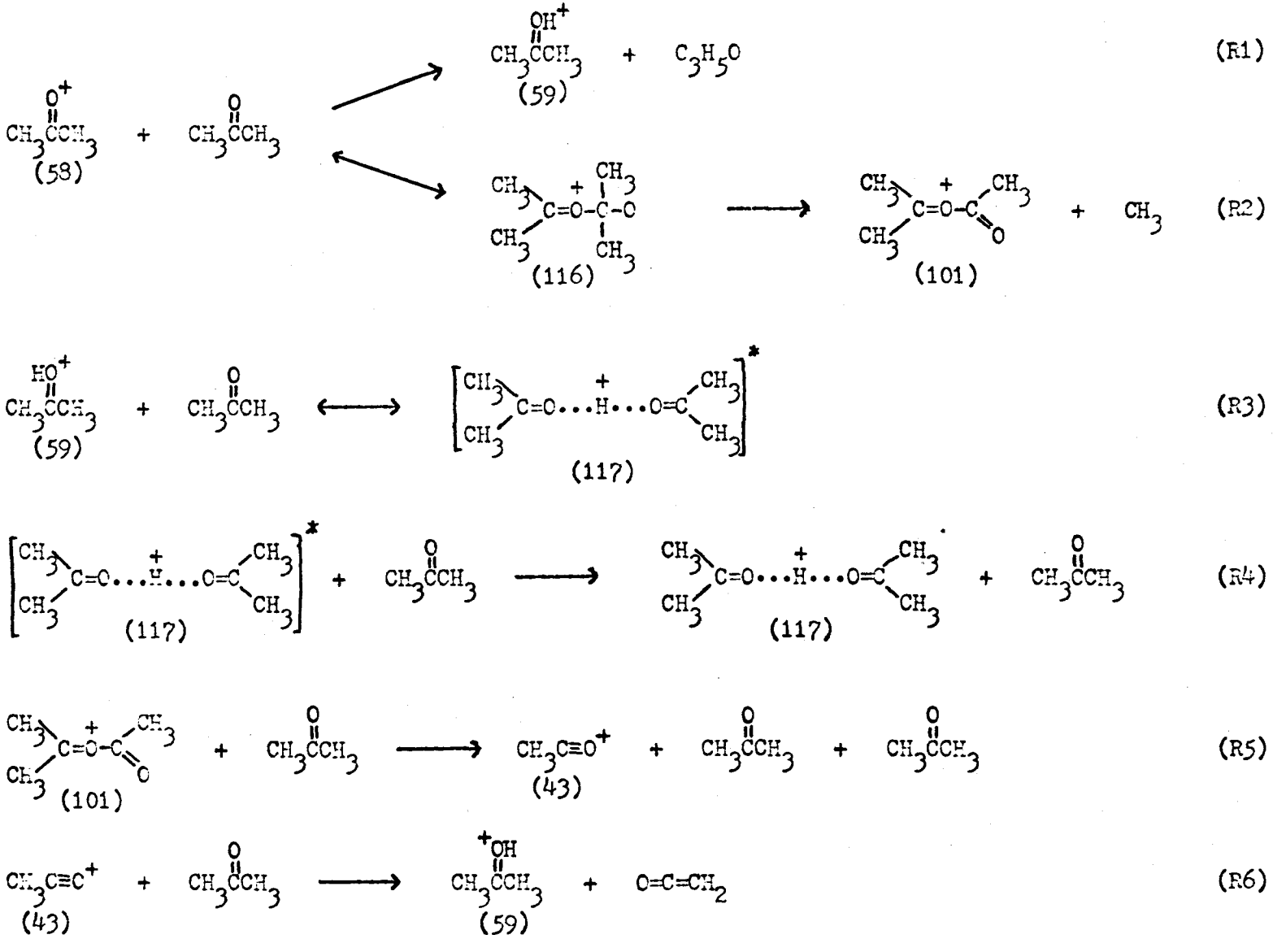

(R1)

(R2)

(R3)

(R4)

(R5)

(R6)

Figure 14 Relative single resonance signal intensities as a function of pressure in propylene oxide by photoionization icr.

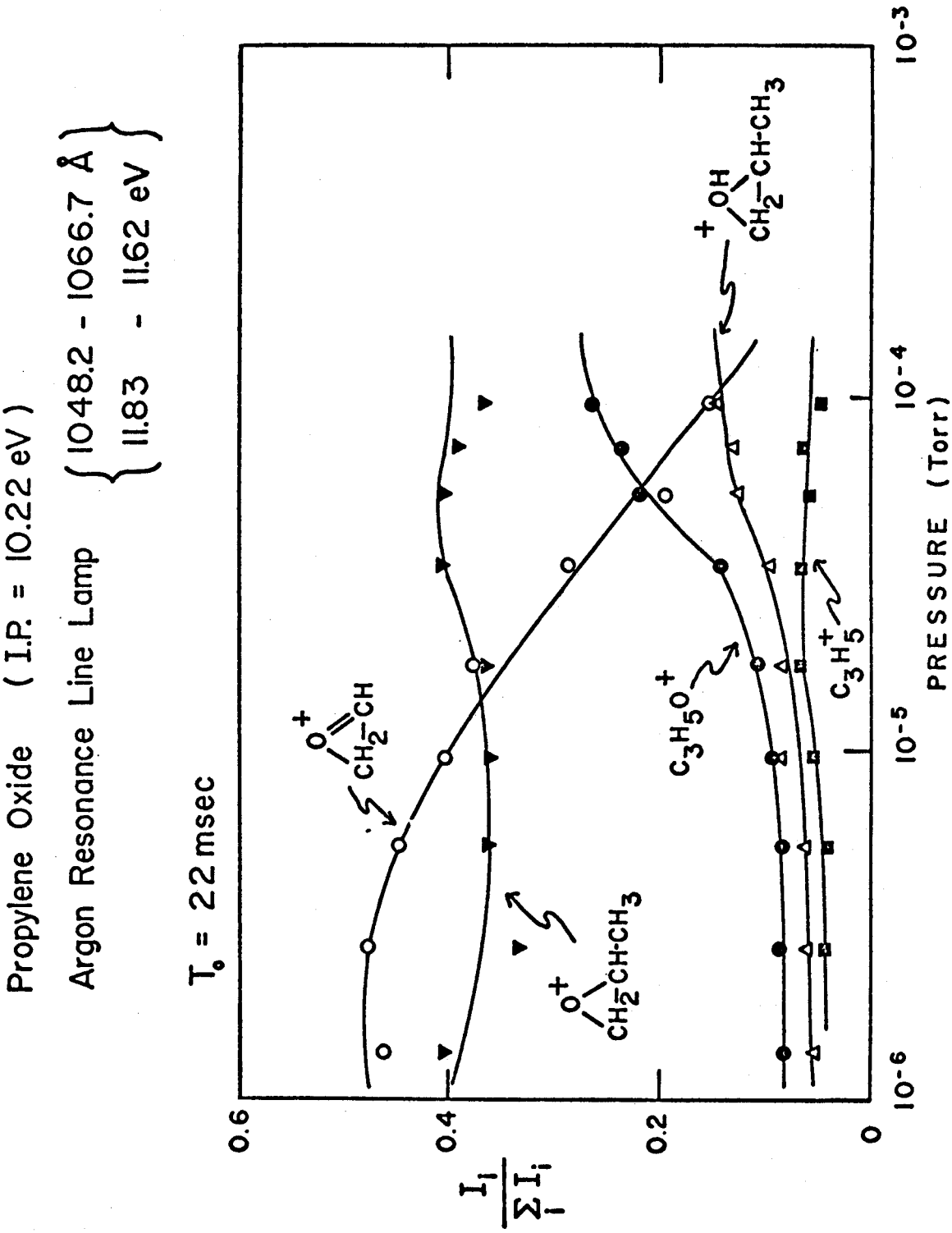
Propylene Oxide (I.P. = 10.22 eV)
Argon Resonance Line Lamp { 1048.2 - 1066.7 Å / 11.83 - 11.62 eV }
T₀ = 22 msec
$\frac{I_i}{\sum I_i}$
0.6
0.4
0.2
0
10^{-6}
10^{-5}
10^{-4}
10^{-3}
PRESSURE (Torr)
O^+ / CH_2=CH
O^+ / CH_2-CH-CH_3
$C_3H_5O^+$
$C_3H_5^+$
+ OH / CH_2-CH-CH_3

Table V Reactions of Propylene Oxide

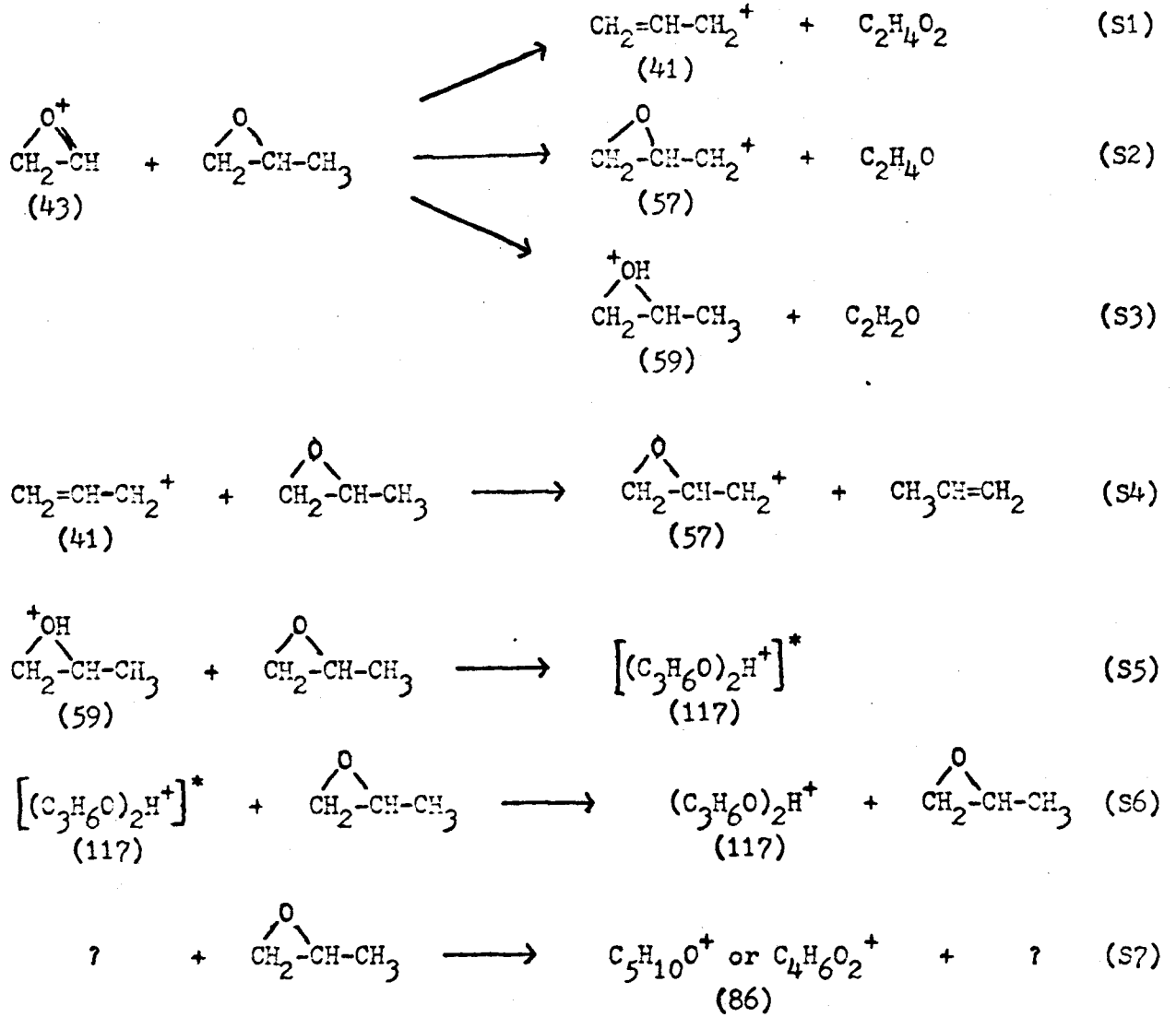

thermodynamically in a reaction converting it to any of the other isomers, especially acetone or propanal. A preliminary investigation of the neutral products of propylene oxide ion-molecule reactions was undertaken using the photolysis cell described earlier.

Propylene oxide was purified on a gas chromatograph and then examined using a flame ionization detector, until a sample with no impurity peaks was obtained. Lamp II was filled with 490 microns argon and its output checked on the monochromator. The ratio of the intensity of the Lyman alpha peak to that of the argon 1067 Å peak (I_{1216}/I_{1067}) was roughly 0.1 after leaving the lamp, and roughly 0.5 after leaving the empty photolysis cell, at 50% radiative power from the microwave generator. It is therefore estimated that inside the cell, the ratio I_{1216}/I_{1067} was in the range 0.25 to 0.35. There were also numerous impurity peaks in the region 1550 Å to 2000 Å (7.9 eV - 6.1 eV), probably due to water contamination (32), with intensities up to 50% of the argon peaks. Thus there was considerable excitation below the ionization potential, as well as ionization by the argon lines.

The photolysis cell and blank were filled with 0.7 torr propylene oxide, as read on a Wallace-Tierman gauge, and the stopcock between the two areas closed. None of the argon lines nor Lyman alpha could be detected passing through the cell containing propylene oxide. A thirty minute photolysis was made, and the lamp then checked again on the monochromator. The impurity lines decreased slightly with use of the lamp. The lamp was still usable one week after filling, with the water peaks reduced to roughly 15% of the argon peaks, and Lyman alpha

increased to roughly 20%. The removal of all stopcock grease from the sealed lamp appears to have solved the severe outgassing problem found in lamp I.

After photolyzing, the cell was attached to the gas chromatograph, with a single β,β'-oxydipropionitrile column, 0.125 in. diameter by ten feet long, leading to a flame ionization detector. The chromatograph showed about $4\frac{1}{2}\%$ conversion of the propylene oxide, with propanal ($3\frac{1}{2}\%$) and acetaldehyde (1%) the major products. There were nine other peaks less than $\frac{1}{2}\%$ of the propylene oxide peak. The propanal and acetaldehyde peaks were identified by their retention times. Positive identification by mass analysis in a mass spectrometer was attempted on another photolyzed sample, but instrument conditions were not good enough to record usable spectra.

Although no intensity measurements have been made for the lamps used here, an order of magnitude estimate of the light output is 10^{13} quanta/sec (14). Since (a) η is probably less than one, (b) a fragment ion (m/e 43) is formed in roughly the same quantity as the parent ion, and (c) the window on the photolysis cell absorbs 25 - 70 percent of the argon emission lines (24), the rate of parent ion formation is probably a factor of ten lower than the light intensity leaving the lamp. A thirty minute photolysis produces perhaps 1.8×10^{15} parent ions. The 0.7 torr of propylene oxide represents 1.2×10^{18} molecules in the cell; a $3\frac{1}{2}\%$ conversion to propanal represents 4×10^{16} molecules. Although this calculation is likely off by an order of magnitude, a chain length of roughly twenty is indicated, and the high yield of propanal in the photolysis appears consistent with a chain process converting propylene oxide to propanal.

CALCULATION OF POWER ABSORPTION IN PHOTOIONIZATION ICR

Ion Production and Concentration

Photoionization ion cyclotron resonance spectroscopy as described in the previous sections has the photon beam traveling down the entire length of the cell, so that ions are formed throughout the cell. Operating with zero drift potentials and using trapping voltage modulation, the only time that effects power absorption and hence signal intensity is T_o, the time for which the trapping plates are positive and hence trapping positive ions. The simplifying approximation that the observing rf electric field is confined to the area between the resonance region drift plates, without fringe effects, will be made. Under these conditions the power absorption expressions will be obtained.

(i) Photon Flux and Ionization Rate

For the purposes of this calculation, it will be assumed that the photon beam is well collimated by the mask at the end of the cell, so that its cross sectional area A is a constant. It is further assumed that the light beam has uniform intensity throughout its cross section, and that the beam points directly down the center of the cell. Letting y be the distance down the resonance region, Beer's law for the photon flux per unit area is

$$I^R(y) = I_0 e^{-\sigma n(d_s + l_c + y)} = I_o^r e^{-\sigma n y},$$

where I_0 is the intensity of the photon beam per unit area just inside the window, and $I_o^r = I_0 e^{-\sigma n(d_s + l_c)}$ photons $sec^{-1} cm^{-2}$ (See Figure 2). As before, n is the number density of neutral molecules, and σ is the

total absorption cross section of the gas. The rate of photon disappearance is then

$$dI^r(y)/dy = -\sigma n I_o^r e^{-\sigma n y} \text{ photons sec}^{-1}\text{cm}^{-3}.$$

If each photon absorbed by the gas produces η primary ions, the total rate of ion formation is

$$R^r(y) = \eta \sigma n I_o^r A e^{-\sigma n y} = n R_o^r e^{-\sigma n y} \text{ ions sec}^{-1}\text{cm}^{-1},$$

where $R_o^r = \eta \sigma A I_o^r$ ions $\text{cm}^2\text{sec}^{-1}$.

(ii) Maximum Trapping Time

At resonance, ions absorb energy from the rf electric field, and the increased kinetic energy of the ions causes the radii of their cycloid motion in the x,y plane to expand. Using the low pressure equation of motion, as on page 3, the radius of an ion's motion, when $\omega_1 = \omega_c$, is $r(t) = cE_1 t/2H$, where t is the time the ion has been at resonance (4). So long as T_o is less than the time needed for the ions to spiral out to the drift plates, no ions will be lost by neutralization on the drift plates. The time necessary for the first ion to spiral out to one of the drift plates is

$$T' = 2Hr_{min}/E_1 c,$$

where r_{min} is the shortest distance between the photon beam and the drift plates. For a photon beam collimated to a rectangular area 13 x 9 mm in the center of a 1 in. square cell and typical values of the parameters, H = 5 kgauss and E_1 = 45 mV/2.54 cm = 5.89×10^{-5} statvolt/cm, the critical time is T' = 4.6 msec: a modulation frequency of 108 Hz would prevent any ions from spiralling out to the drift plates. When working with ions of mass 20 amu or above and the normal rf power level

of 17.7 mV/cm, a modulation frequency of 260 Hz should be high enough to keep ions from being lost. In cases where the photon beam is not well collimated, so that it diverges appreciably in the resonance region, perhaps even striking the drift plates, explicit correction for ion neutralization must be included in the power absorption expression. Trapping periods slightly longer than the shortest T' of a given scan should give increased signal intensities, without greatly affecting the relative signal strength.

(iii) Reaction Rates and Population Figures

This first treatment of photoionization icr will deal with the relatively simple system, one primary ion P^+ reacting to form one secondary ion S^+, which reacts to form a tertiary ion T^+. Consider a closed volume V, with a neutral gas density of n molecules/cm^3, in which there are $P^+(0)$ primary ions present at t = 0, and no secondary or tertiary ions. The ion population in V will satisfy the following differential equations:

$$dP^+(t)/dt = -nk_1P^+(t),$$

$$dS^+(t)/dt = nk_1P^+(t) - nk_2S^+(t),$$

$$dT^+(t)/dt = nk_2S^+(t),$$

where k_i is a bimolecular rate constant, units $cm^3sec^{-1}molecule^{-1}$. These differential equations have as solutions, with $S^+(0) = T^+(0) = 0$,

$$P^+(t) = P^+(0)e^{-nk_1t},$$

$$S^+(t) = P^+(0)k_1(e^{-nk_2t} - e^{-nk_1t})/(k_1 - k_2),$$

$$T^+(t) = P^+(0)k_1k_2\{(1 - e^{-nk_2t})/k_2 - (1 - e^{-nk_1t})/k_1\}/(k_1 - k_2).$$

The resonance region of the cell has a cross section of B cm^2, and in the center of it, a region of A cm^2 in which ions are formed. In the

small volume Bdy, there are $R^r(y)dy$ ions/sec formed; in the short interval dt there are $R^r(y)dydt$ ions formed. All the ions formed by photon impact are primary ions in this model, and constitute an ion population which satisfies the above equations. All ions formed in the differential space-time volume Bdydt can be considered as having been formed at the same instant of time.

At a time τ after the $P^+(0) = R^r(y)dydt$ primary ions were formed in Bdydt, there will be $P^+(\tau) = R^r(y)dydte^{-nk_1\tau}$ primary ions remaining, the residuum having reacted to form secondary ions. The total number of primary ions in the cell at a time T after the trapping voltage goes positive ($T<T_o$) is

$$n_p^+(T) = \int_0^T \int_0^{l_r} nR_o^r e^{-nk_1\tau} e^{-\sigma ny}\, dydt = D_1/k_1\ (1 - e^{-nk_1T}),$$

where $D_1 = R_o^r \frac{(1 - e^{-\sigma nl_r})}{n\sigma}$. The following diagram shows the sequence of events:

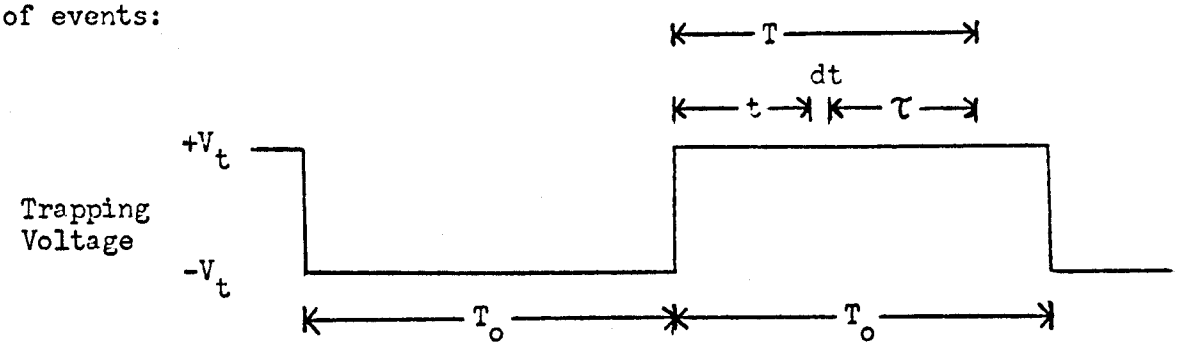

Calculating the secondary and tertiary ion populations in an analagous manner, the product ion populations at the time T are

$$n_S^+(T) = D_1k_1\{(1 - e^{-nk_2T})/k_2 - (1 - e^{-nk_1T})/k_1\}/(k_1 - k_2);$$

$$n_T^+(T) = D_1k_1k_2\{(nk_2T - 1 + e^{-nk_2T})/k_2^2 - (nk_1T - 1 + e^{-nk_1T})/k_1^2\}/(k_1 - k_2).$$

The sum of the ion populations at a time T is D_1nT. A graph of the relavite ion populations as a function of n is given in Figure 15.

Figure 15 Theoretical relative ion abundances as a function of pressure in photoionization icr. Trapping modulation used with zero drift potentials. Calculated for the system

$$P^+ \xrightarrow{k_1} S^+ \xrightarrow{k_2} T^+$$

with $k_1 = 3.0 \times 10^{-10}$ $cm^3 sec^{-1}$ $molecule^{-1}$ and $k_2 = 2.0 \times 10^{-10}$ $cm^3 sec^{-1} molecule^{-1}$.

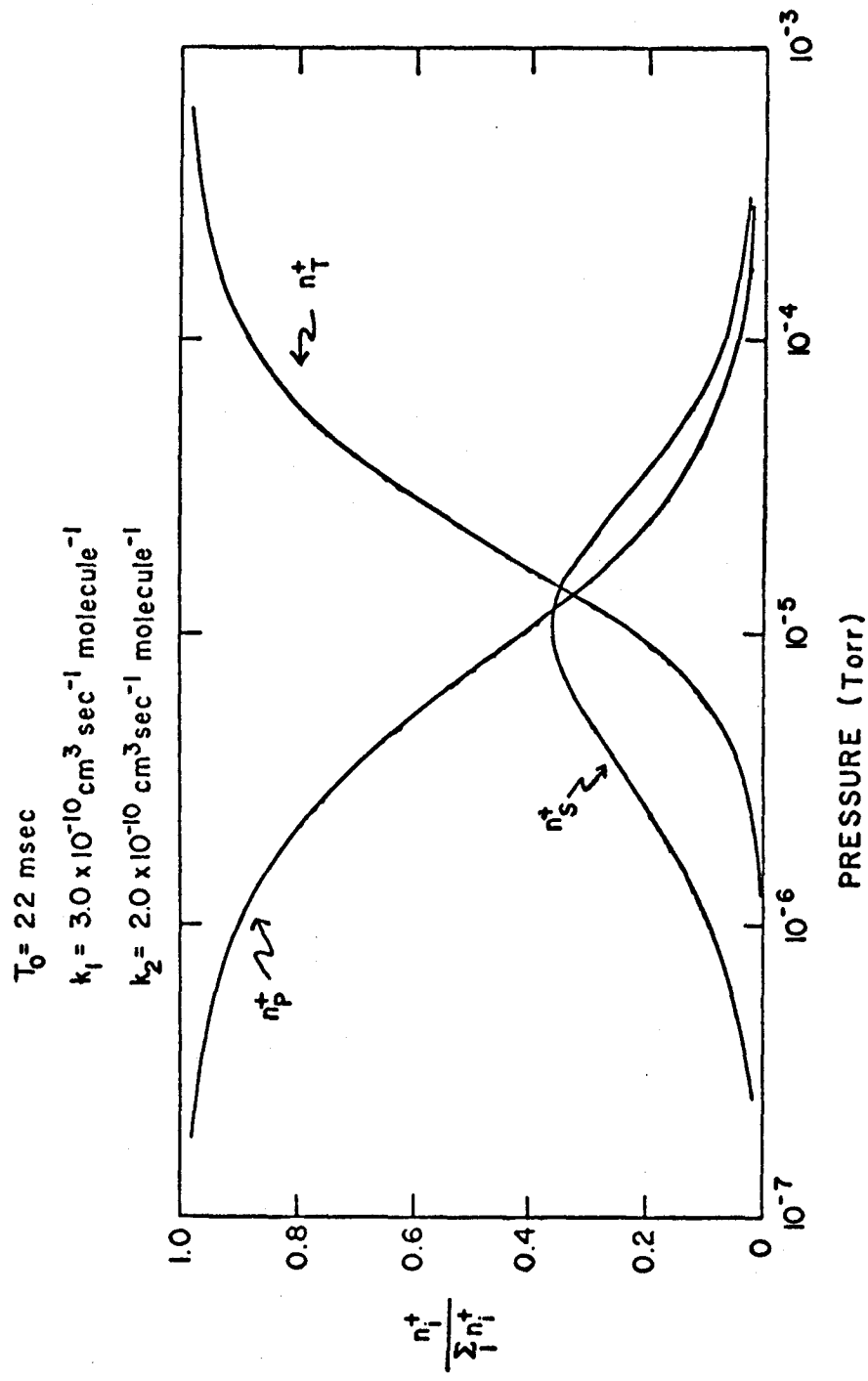
T_0= 22 msec
k_1= 3.0 x 10^{-10} cm^3 sec^{-1} molecule^{-1}
k_2= 2.0 x 10^{-10} cm^3 sec^{-1} molecule^{-1}
n_T^+
n_P^+
n_S^+
$\frac{n_i^+}{\sum_i n_i^+}$
1.0
0.8
0.6
0.4
0.2
0
10^{-7}
10^{-6}
10^{-5}
10^{-4}
10^{-3}
PRESSURE (Torr)

Power Absorption and Signal Intensity

(i) Instantaneous Power Absorption

At low pressures, where the simplified power absorption expression derived in the introduction can be used to a good approximation, the power absorption will be limited by the time the ions are trapped, for we are assuming $T_o < T'$ for all ions P^+, S^+, and T^+.

Consider again the infinitesimal space-time volume Bdydt: after a time τ there will be $nR_o^r e^{-\sigma n y} e^{-nk_1\tau} dydt$ primary ions remaining, all of which will be absorbing power at the rate $A(m_p,\tau) = q^2E_1^2\tau/4m_p$. The power absorption at a time $T = t + \tau$ due to primary ions formed in Bdydt is

$$dA_p(T,t,y) = nR_o^r e^{-\sigma n y} e^{-nk_1\tau} q^2E_1^2\tau/4m_p \, dydt.$$

Making the subsitution $\tau = T - t$, the total primary ion power absorption at the instant T is

$$A_p(T) = \int_0^T \int_0^{l_r} dA_p(T,t,y) = C_1(1 - e^{-nk_1T} - nk_1Te^{-nk_1T})/m_pk_1^2,$$

where $C_1 = R_o^r q^2 E_1^2 (1 - e^{-\sigma n l_r})/4\sigma n^2$.

Note that we assume that an ion, when at resonance, has been absorbing power since it was formed. Thus there is no unique reaction constant k that describes its reactivity; rather, the rate of reaction over an energy range from thermal to that achieved at maximum power absorption is sampled. This effect is noticed more in photoionization icr, since there is no source region residence time free of the observing oscillator as in electron impact icr.

The case of secondary ion power absorption is complicated because all secondary ions coming from primary ions formed in Bdydt have not been

absorbing power for the same length of time at resonance. Using the following diagram to define times, consider the $nR_o^r e^{-\sigma ny} dydt$ primary

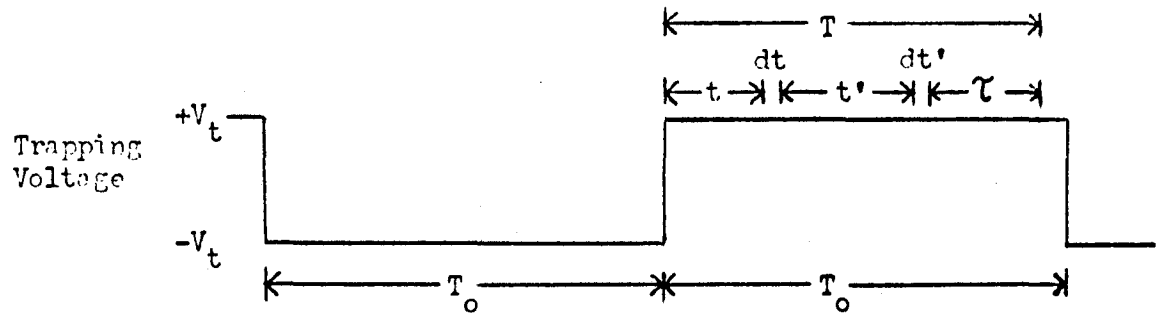

ions formed in Bdydt. The rate of formation of secondary ions at a time t' later is $dS^+(t')/dt' = nk_1 P^+(t')$. Thus in the infinitesimal time dt' there are $dS^+(t') = nk_1(nR_o^r e^{-\sigma ny} dydt)e^{-nk_1 t'}dt'$ secondary ions formed. At a time τ later, there are $dS^+(t')e^{-nk_2\tau}$ secondary ions remaining; they have been absorbing power for a time τ. The instantaneous power absorption of an ion at $T = t + t' + \tau$ is $A(m_S,\tau) = q^2 E_1^{\,2}\tau/4m_S$. The instantaneous power absorption at T arising from secondary ions formed in dt' coming from primary ions formed in dt is

$$dA_S(T,t',t,y) = nk_1(nR_o^r e^{-\sigma ny} dydt)e^{-nk_1 t'}dt'(q^2 E_1^{\,2}\tau/4m_S)e^{-nk_2\tau}.$$

The total instantaneous power absorption of all secondary ions at T is

$$A_S(T) = \int_0^T \int_0^{T-t} \int_0^{l_r} dA_S(T,t',t,y)$$

$$= \frac{C_1}{m_S(k_1 - k_2)^2}\left\{1 - e^{-nk_1 T} + \frac{k_1}{k_2}\left[2 - \frac{k_1}{k_2}\right]\left(e^{-nk_2 T} - 1\right) - \frac{k_1}{k_2}(k_1 - k_2)nTe^{-nk_2 T}\right\}.$$

The tertiary ion power absorption is somewhat easier to derive. From the $nR_o^r e^{-\sigma ny} dydt$ primary ions formed in Bdydt, the rate of tertiary ion formation a time t' later is $dT^+(t')/dt' = nk_2 S^+(t')$, and in the

interval dt' there are $dT^+(t') = nk_2S^+(t')dt'$ tertiary ions formed. For an unreactive tertiary ion, all of these ions will be absorbing power at the same rate, $A(m_T,\tau)$, at a time τ later. So the instantaneous power absorption of tertiary ions at $T = t + t' + \tau$, formed in dt' from primary ions formed in Bdydt, is

$$dA_T(T,t,t',y) = nk_2(nR_o^r e^{-\sigma ny}dydt)\frac{k_1}{(k_1 - k_2)}(e^{-nk_2t'} - e^{-nk_1t'})q^2E_1^2\tau/4m_T.$$

The total instantaneous power absorption from all tertiary ions at T is

$$A_T(T) = \int_0^T\int_0^{T-t}\int_0^{l_r} dA_T(T,t,t',y)$$

$$= \frac{C_1}{m_T(k_1 - k_2)}\left[\frac{k_1}{k_2}^2\left\{\tfrac{1}{2}(nk_2T)^2 - e^{-nk_2T} + 1 - nk_2T\right\}\right.$$

$$\left. - \frac{k_2}{k_1}^2\left\{\tfrac{1}{2}(nk_1T)^2 - e^{-nk_1T} + 1 - nk_1T\right\}\right].$$

The case of a reactive tertiary ion is not generally considered, since it is usually difficult to detect usefully any terniary products, due to decreasing resolution at higher pressures and the usually large mass number involved.

In photoionization icr, the instantaneous power absorption depends on T, the time the trapping voltage has been positive. In electron impact icr, where ions are drifted from the source to the analyzer region, the instantaneous power absorption reaches a steady value after the first ion crosses the resonance region. When the magnetic field is swept to bring the cyclotron frequency of each ion into resonance with the fixed frequency rf observing oscillator, each ion will have a different drift velocity at its resonance magnetic field, and hence a different residence time in the analyzer region. Thus, in electron impact icr, the power absorption expressions contain exponentials that depend on the ion mass.

(ii) Detector Output

The time varying output of the marginal oscillator detection system is not recorded directly, but is fed through a phase sensitive detector tuned to the trapping voltage modulation frequency. The output of the phase sensitive detector is the integral of the instantaneous power absorption from T = 0 to T = T_o. The detector output for primary, secondary, and tertiary ions is

$$I_P = \frac{C_1}{(m_P n k_1^3)} \left\{ 2e^{-nk_1T_o} - 2 + nk_1T_o + nk_1T_o e^{-nk_1T_o} \right\} ;$$

$$I_S = \frac{C_1}{m_S n (k_1 - k_2)^2 k_1} \left[nk_1T_o + e^{-nk_1T_o} - 1 + \frac{k_1}{k_2}\left(2 - \frac{k_1}{k_2}\right)\left[\frac{k_1}{k_2} - nk_1T_o - \frac{k_1}{k_2} e^{-nk_2T_o}\right] + \frac{k_1^2(k_1 - k_2)}{k_2^3}\left\{nk_2T_o e^{-nk_2T_o} + e^{-nk_2T_o} - 1\right\}\right] ;$$

$$I_T = \frac{C_1}{m_T n (k_1 - k_2) k_1 k_2} \left\{ \frac{k_1^2}{k_2^2}\left[\frac{(nk_2T_o)^3}{6} + e^{-nk_2T_o} - 1 + nk_2T_o - \frac{(nk_2T_o)^2}{2}\right] - \frac{k_2^2}{k_1^2}\left[\frac{(nk_1T_o)^3}{6} + e^{-nk_1T_o} - 1 + nk_1T_o - \frac{(nk_1T_o)^2}{2}\right]\right\}.$$

Figure 16 is a graph of relative signal intensity as a function of pressure for typical values of k_1 and k_2.

Figure 16 Theoretical relative single resonance signal intensities as a function of pressure in photoionization icr. Calculated for the system

$$P^+ \xrightarrow{k_1} S^+ \xrightarrow{k_2} T^+$$

with $k_1 = 3.0 \times 10^{-10}$ $cm^3 sec^{-1} molecule^{-1}$ and $k_2 = 2.0 \times 10^{-10}$ $cm^3 sec^{-1} molecule^{-1}$. Comparison with Figure 15 shows that the icr signal "lags" the true ion concentration.

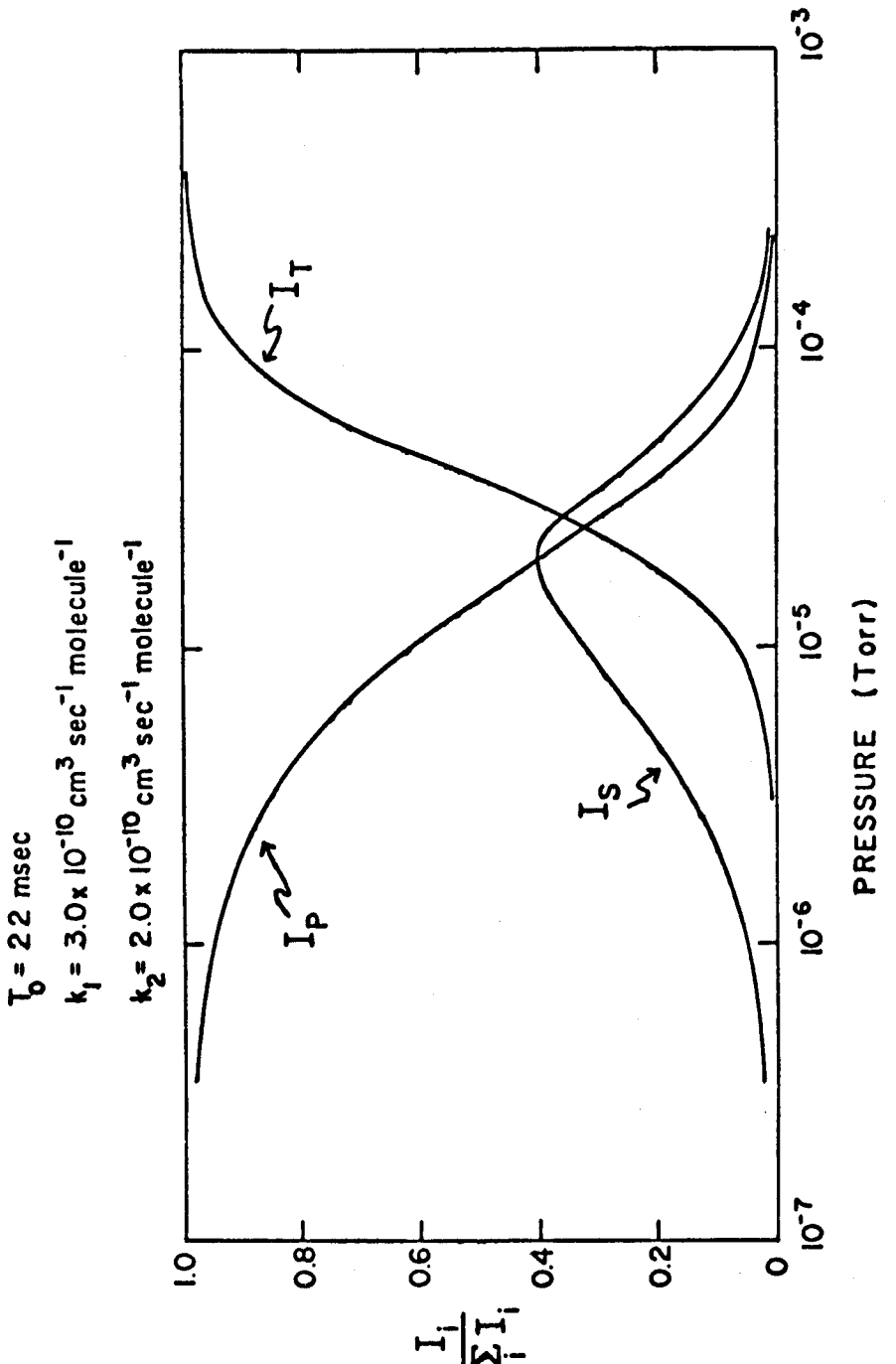
τ_b = 2.2 msec
k_1 = 3.0 x 10^{-10} cm^3 sec^{-1} molecule^{-1}
k_2 = 2.0 x 10^{-10} cm^3 sec^{-1} molecule^{-1}
I_T
I_P
I_S
$\frac{I_i}{\sum_i I_i}$
1.0
0.8
0.6
0.4
0.2
0
10^{-7}
10^{-6}
10^{-5}
10^{-4}
10^{-3}
PRESSURE (Torr)

Lineshape for the Case of a Non-reactive Primary Ion

The previous calculations were performed for the condition of resonant power absorption. However, it is also useful to calculate the frequency dependent lineshape and to compare it with experiment. The following derivation treats a non-reactive primary ion.

The kinetic energy of an ion in the x,y plane of the spectrometer, where the magnetic field is in the -z direction, under the influence of an irradiating rf electric field $E_1 \sin\omega_1 t$, is (33)

$$E_{ion}(t) = \tfrac{1}{2}m(v_x^2 + v_y^2) = \frac{q^2E_1^2\left[1 - \cos\{(\omega_1 - \omega_c)t\}\right]}{4m(\omega_1 - \omega_c)^2}$$

$$= \frac{q^2E_1^2 \sin^2\{\frac{1}{2}(\omega_1 - \omega_c)t\}}{2m(\omega_1 - \omega_c)^2},$$

where t is the time the ion has been in the rf electric field. The initial position, velocity, and phase difference between the ion's cyclotron motion and the rf electric field have been neglected, as they will average out to zero. The power absorption is the time derivative of the kinetic energy:

$$A(m,t) = dE_{ion}(t)/dt = \frac{q^2E_1^2 \sin\{(\omega_1 - \omega_c)t\}}{4m(\omega_1 - \omega_c)}.$$

The total instantaneous power absorption arising from all primary ions after the trapping voltage has been positive for a time T is

$$A^+(T,\omega_c) = \int_0^T \int_0^{l_r} \frac{q^2E_1^2 n R_o^r}{4m} e^{-\sigma ny} \frac{\sin\{(\omega_1 - \omega_c)(T - t)\}}{(\omega_1 - \omega_c)} dydt$$

$$= \frac{q^2E_1^2R_o^r (1 - e^{-\sigma nl_r})}{2\sigma m} \frac{\sin^2\{\frac{1}{2}(\omega_1 - \omega_c)T\}}{(\omega_1 - \omega_c)^2}.$$

The detector output is the time integral of the instantaneous power absorption over the time the trapping plate is positive, T_o:

$$I^+(T_o,\omega_c) = \frac{q^2E_1{}^2R_o^r\,(1 - e^{-\sigma nl_r})}{4\sigma m}\,\frac{\left[(\omega_1 - \omega_c)T_o - \sin\{(\omega_1 - \omega_c)T_o\}\right]}{(\omega_1 - \omega_c)^3}\,.$$

As the magnetic field is swept to bring each ion into resonance with the fixed observing field, it is $\omega_c = qH/mc$ that varies.

At resonance, $\omega_c = \omega_1$, and the power absorption of an individual ion reduced to $A(m,t) = q^2E_1{}^2t/4m$. The detector output is then

$$I^+(T_o,\omega_1) = \int_0^T\int_0^{T_o}\int_0^{l_r} \frac{q^2E_1{}^2nR_o^r e^{-\sigma ny}}{4m}\,(T - t)\,dydtdT$$

$$= \frac{q^2E_1{}^2R_o^r\,(1 - e^{-\sigma nl_r})}{4\sigma m}\,\frac{T_o{}^3}{6}\,.$$

This is the limit of the full ω_c-dependent signal intensity at $\omega_c = \omega_1$.

If we let $z = (\omega_1 - \omega_c)T_o$, the half-width at half-height, $(\omega_1 - \omega_c)_{\frac{1}{2}}$, is found from the solution of the equation

$$z - \sin z = z^3/12.$$

This can be solved to yield $z = 3.70554$, or $(\omega_1 - \omega_c)_{\frac{1}{2}} = 3.70554/T_o$. At a trapping frequency of 100 Hz, or a trapping time of $T_o = 5$ msec, this would give $(\omega_1 - \omega_c)_{\frac{1}{2}} = 741.1\ \text{sec}^{-1}$. For a normal operating frequency of the marginal oscillator, corresponding to 100 gauss/amu, where ω_1 is $9.64 \times 10^5\ \text{sec}^{-1}$, and for an ion of mass 30, the peak width at half height is

$$2(H - H_c)_{\frac{1}{2}} = 2(\omega_1 - \omega_c)_{\frac{1}{2}}\,H_c/\omega_1 = 4.62 \text{ gauss},$$

where H_c is the resonance magnetic field, in this case, 3 Kgauss.

A graph of the theoretical lineshape is given in Figure 17, where $H = mc\omega_c/q$ has been used as the ordinate. As can be seen, the lineshape

Figure 17 Theoretical lineshape for a non-reactive primary ion by photoionization icr with zero drift potentials and trapping voltage modulation. Calculated for low pressures where collisions with neutral molecules occur with lower frequency than the square wave trapping voltage frequency.

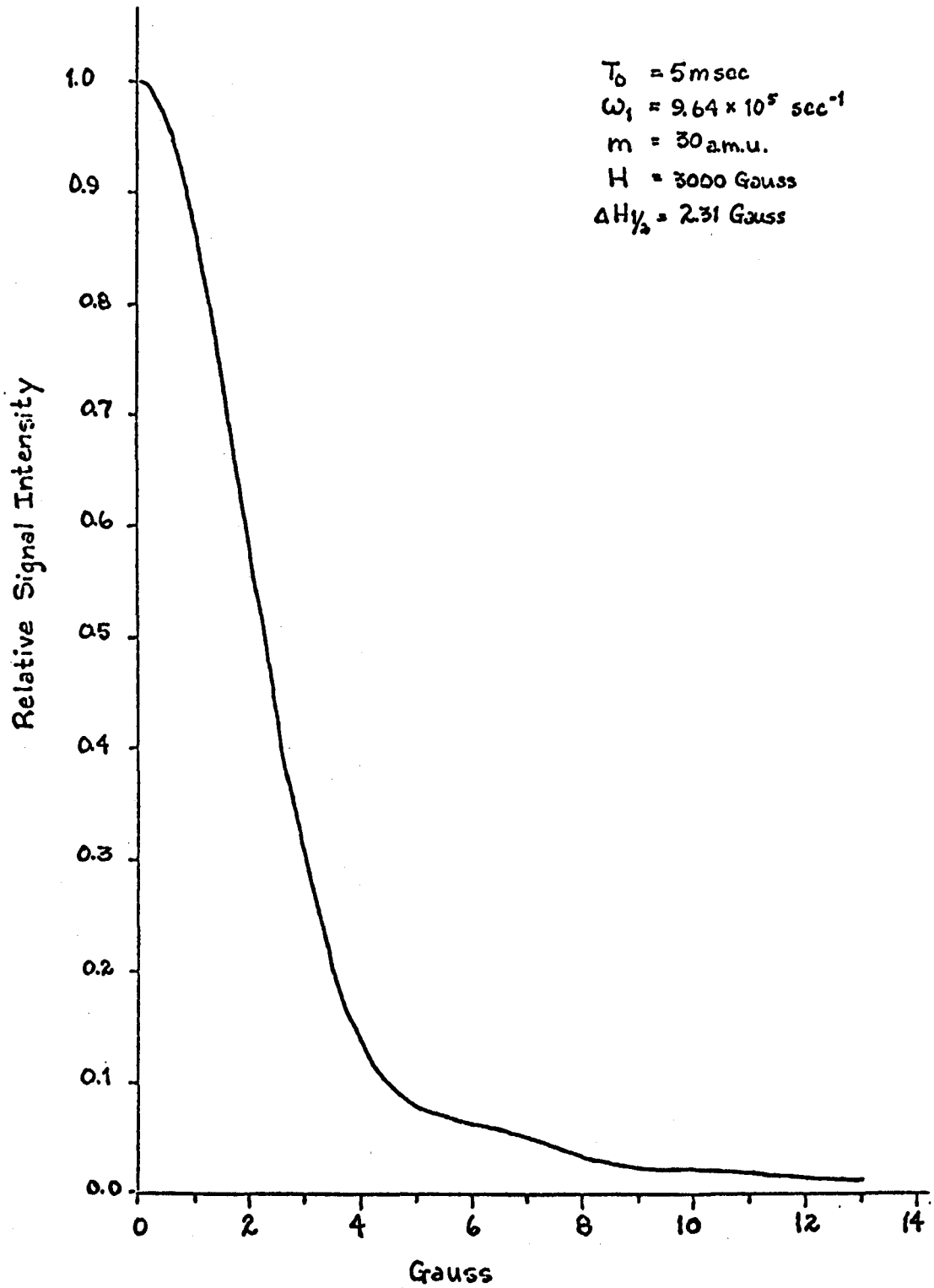
T_0 = 5 msec
ω_1 = 9.64 × 10^5 sec^{-1}
m = 30 a.m.u.
H = 3000 Gauss
$\Delta H_{1/2}$ = 2.31 Gauss
Relative Signal Intensity
1.0
0.9
0.8
0.7
0.6
0.5
0.4
0.3
0.2
0.1
0.0
0
2
4
6
8
10
12
14
Gauss

does not have many prominent features, and it will probably be impossible to see the small detail in the skirt of the curve. A better check on the experimental agreement with the calculated lineshape would be varying the trapping period T_o and observing the change in half-width; plotting half-width vs. $1/T_o$ should yield a straight line. Specifically, the full peak width at half height should be

$$2(H - H_c)_{\frac{1}{2}} = 7.68784 \times 10^{-6} \quad \frac{H_c}{T_o \text{ sec}^{-1}} \cdot$$

The half-width is thus also directly proportional to magnetic field.

This calculation yields the residence time limited expression for the lineshape, with no collisions between ions and neutral molecules. The effect of collisions interrupting the power absorption of ions (pressure broadening) could be seen by considering an equation of motion with a factor expressing momentum loss due to ion-neutral collisions.

REFERENCES

1. H. Somer, H. A. Thomas, and J. A. Hipple, Phys. Rev., 76, 1877 (1949).

2. J. L. Beauchamp, J. Chem. Phys., 46, 1231 (1967).

3. J. T. Armstrong and J. L. Beauchamp, Rev. Sci. Inst., 40, 123 (1969).

4. J. L. Beauchamp, Ph. D. Thesis, Harvard University, 1967.

5. D. Wobschall, J. R. Graham, and D. P. Malone, Phys. Rev., 131, 1565 (1963).

6. R. C. Dunbar, J. Chem. Phys., 54, 711 (1971).

7. J. L. Beauchamp, Ann. Rev. Phys. Chem., 22, 527 (1971).

8. R. W. Kiser, Introduction to Mass Spectroscopy and Its Applications, (Prentice Hall, Englewood Cliffs, New Jersey, 1965).

9. J. C. Person and P. P. Nicole, J. Chem. Phys., 49, 5421 (1968).

10. C. E. Klotz, Fundamental Processes in Radiation Chemistry, edited by P. Ausloos, (Wiley, New York, 1968).

11. J. C. Person and P. P. Nicole, Argonne National Laboratory Radiological Physics Division Annual Report, July 1967 through June 1968. ANL-7489.

12. D. P. Ridge and J. L. Beauchamp, J. Chem. Phys., 51, 470 (1969).

13. J. A. R. Sampson, Techniques of Vacuum Ultraviolet Spectroscopy, (Wiley, New York, 1967).

14. A. L. Lane and A. Kuppermann, Rev. Sci. Inst., 22, 126 (1968).

15. R. Gordon, R. E. Rebbert, and P. Ausloos, Rare Gas Resonance Lamps, National Bureau of Standards Technical Note 496 (U. S. Government Printing Office, Washington, D. C., 1969).

16. A. L. Lane, private communication.

17. D. P. Ridge, private communication.

18. R. H. Wyatt and J. L. Beauchamp, private communication.

19. E. Murad and M. G. Inghram, J. Chem. Phys., 40, 3263 (1964).

20. P. F. Knewstubb, Mass Spectrometry and Ion Molecule Reactions, (Cambridge University Press, Cambridge, England, 1969).

21. W. A. Chupka, J. Chem. Phys., 30, 191 (1959).

22. (a) W. S. Updegrove, J. Cro, and A. Zlatkis, Adv. Gas Chromatog., 4, 82 (1967); (b) J. Throck Watson, Ancillary Techniques of Gas Chromatography, edited by L. Ettre and W. McFadden, (Wiley-Interscience, New York, 1969); (c) A. L. Lane, Ph. D. Thesis, University of Illinois, 1969; (d) P. S. Gill, Y. Inel, and G. G. Meisels, J. Chem. Phys., 54, 2811 (1971).

23. (a) L. H. Gevantman and R. R. Williams, J. Phys. Chem., 56, 569 (1952); (b) P. Ausloos and S. G. Lias, J. Chem. Phys., 44, 521 (1966); (c) L. I. Bone and J. H. Futrell, J. Chem. Phys., 47, 4366 (1967).

24. A. H. Laufer, J. A. Pirog, and J. R. McNesby, J. Opt. Soc. Am., 55, 64 (1965).

25. P. Warneck, J. Opt. Soc. Am., 55, 921 (1965).

26. R. Allison, J. Burns, and A. J. Tuzzolino, J. Opt. Soc. Am., 54, 747 (1964).

27. R. A. Knapp, Appl. Opt., 2, 1234 (1963).

28. J. Diekman, J. K. McLeod, C. Djerrassi, and J. D. Baldeschwieler, J. Am. Chem. Soc., 91, 2069 (1969).

29. J. L. Beauchamp and R. C. Dunbar, J. Am. Chem. Soc., 92, 1477 (1970).

30. J. L. Franklin, J. G. Dillard, H. M. Rosenstock, J. T. Herron, K. Draxl, and F. H. Field, Ionization Potentials, Appearance Potentials, and Heats of Formation of Gaseous Positive Ions, NSRDS-NBS 26, (U. S. Government Printing Office, Washington, D.C., 1969).

31. S. W. Benson, Thermochemical Kinetics, (Wiley, New York, 1968).

32. H. Okabe, J. Opt. Soc. Am., 54, 478 (1964).

33. S. E. Buttrill, J. Chem. Phys., 50, 4125 (1969).